USAAMRDL TECHNICAL REPORT 71-37

DESIGN AND EVALUATION OF ADVANCED HIGH-SPEED FUEL PUMP

By

Harry T. Johnson

July 1971

EUSTIS DIRECTORATE
U. S. ARMY AIR MOBILITY RESEARCH AND DEVELOPMENT LABORATORY
FORT EUSTIS, VIRGINIA

CONTRACT DAAJ02-69-C-0072
BATTELLE
COLUMBUS LABORATORIES
COLUMBUS, OHIO

DISCLAIMERS

The findings in this report are not to be construed as an official Department of the Army position unless so designated by other authorized documents.

When Government drawings, specifications, or other data are used for any purpose other than in connection with a definitely related Government procurement operation, the United States Government thereby incurs no responsibility nor any obligation whatsoever; and the fact that the Government may have formulated, furnished, or in any way supplied the said drawings, specifications, or other data is not to be regarded by implication or otherwise as in any manner licensing the holder or any other person or corporation, or conveying any rights or permission, to manufacture, use, or sell any patented invention that may in any way be related thereto.

DISPOSITION INSTRUCTIONS

Destroy this report when no longer needed. Do not return it to the originator.

Unclassified

Security Classification

DOCUMENT CONTROL DATA - R & D

(Security classification of title, body of abstract and indexing annotation must be entered when the overall report is classified)

1. ORIGINATING ACTIVITY (Corporate author) Battelle, Columbus Laboratories 505 King Avenue Columbus, Ohio	2a. REPORT SECURITY CLASSIFICATION Unclassified 2b. GROUP

3. REPORT TITLE

DESIGN AND EVALUATION OF ADVANCED HIGH-SPEED FUEL PUMP

4. DESCRIPTIVE NOTES (Type of report and inclusive dates)

Final Technical Report

5. AUTHOR(S) (First name, middle initial, last name)

Harry T. Johnson

6. REPORT DATE	7a. TOTAL NO. OF PAGES	7b. NO. OF REFS
July 1971	62	1

8a. CONTRACT OR GRANT NO. DAAJ02-69-C-0072 b. PROJECT NO. Task 1G162203D14416 c. d.	9a. ORIGINATOR'S REPORT NUMBER(S) USAAMRDL Technical Report 71-37 9b. OTHER REPORT NO(S) (Any other numbers that may be assigned this report)

10. DISTRIBUTION STATEMENT

Approved for public release; distribution unlimited.

11. SUPPLEMENTARY NOTES	12. SPONSORING MILITARY ACTIVITY Eustis Directorate U.S.Army Air Mobility Research and Development Laboratory Fort Eustis, Virginia

13. ABSTRACT The purpose of this program was to develop both the technology and the experimental hardware to experimentally demonstrate that a main-engine fuel pump could be operated at turbine-engine shaft speeds. A single-lobe vane pump has been designed and successfully operated at speeds up to 49,500 rpm and outlet pressures up to 900 psig while pumping JP-4 turbine fuel. The promising capabilities demonstrated by this pump were the result of the successful application of hydrodynamic lubrication techniques to the vane design. The pivoting vane tip concept incorporated permits tip surface speeds up to 180 fps to be achieved without producing high mechanical power losses or sacrificing the pump endurance capabilities.

The experimental fuel pump has met the design flow-rate requirement of 2000 lb/hr at 650 psig and the 100-percent speed of 40,000 rpm. It has successfully completed a 200-hour endurance evaluation at speeds from 26,000 to 40,000 rpm with virtually no degradation in the performance parameters. A total of 34 hours of operation with fuel contaminated per MIL-E-5007C has been accomplished without experiencing pump mechanical failure. The flow performance was unacceptable after 34 hours, however, and the results suggest that tungsten carbide vane-stage components will be required to establish the capability to withstand long-term exposure to the contaminated environment.

The present experimental fuel pump represents a significant step toward the development of flight hardware capable of operating at engine shaft speed. It meets the basic performance requirements of a main-engine fuel pump typically required on small, high-speed gas-turbine engines. In addition, it appears that a variable-displacement capability could be developed directly from the present hardware without altering the established high-speed capabilities.

DD FORM 1 NOV 68 1473 REPLACES DD FORM 1473, 1 JAN 64, WHICH IS OBSOLETE FOR ARMY USE.

Unclassified

Security Classification

14. KEY WORDS	LINK A		LINK B		LINK C	
	ROLE	WT	ROLE	WT	ROLE	WT
pump						
vane						
centrifugal						
fuel						
high-speed						
turbine-speed						
single-lobe vane pump						
pivoting-tip vane						
centrally pivoted pad bearings						
hydrodynamic lubrication						
inner vane						

DEPARTMENT OF THE ARMY
U. S. ARMY AIR MOBILITY RESEARCH & DEVELOPMENT LABORATORY
EUSTIS DIRECTORATE
FORT EUSTIS, VIRGINIA 23604

The research described herein was performed by Battelle Memorial Institute under U. S. Army Contract DAAJ02-69-C-0072. The work was conducted under the technical management of Mr. R. G. Furgurson, Propulsion Division, Eustis Directorate, USAAMRDL.

Appropriate technical personnel of this Directorate have reviewed this report and concur with the findings and conclusions contained herein.

The recommendations set forth in this report will be considered in planning any future programs of high-speed pump development.

Task 1G162203D14416
Contract DAAJ02-69-C-0072
USAAMRDL Technical Report 71-37
July 1971

DESIGN AND EVALUATION OF ADVANCED HIGH-SPEED FUEL PUMP

Final Report

by

Harry T. Johnson

Prepared by

BATTELLE
Columbus Laboratories
Columbus, Ohio

for

EUSTIS DIRECTORATE
U. S. ARMY AIR MOBILITY RESEARCH AND DEVELOPMENT LABORATORY
FORT EUSTIS, VIRGINIA

SUMMARY

The purpose of this program was to develop both the technology and the experimental hardware to experimentally demonstrate that a main-engine fuel pump could be operated at turbine-engine shaft speeds. A single-lobe vane pump has been designed and successfully operated at speeds up to 49,500 rpm and outlet pressures up to 900 psig while pumping JP-4 turbine fuel. The promising capabilities demonstrated by this pump were the result of the successful application of hydrodynamic lubrication techniques to the vane design. The pivoting vane tip concept incorporated permits tip surface speeds up to 180 fps to be achieved without producing high mechanical power losses or sacrificing the pump endurance capabilities.

The experimental fuel pump has met the design flow-rate requirement of 2000 lb/hr at 650 psig and the 100-percent speed of 40,000 rpm. It has successfully completed a 200-hour endurance evaluation at speeds from 26,000 to 40,000 rpm with virtually no degradation in the performance parameters. A total of 34 hours of operation with fuel contaminated per MIL-E-5007C has been accomplished without experiencing pump mechanical failure. The flow performance was unacceptable after 34 hours, however, and the results suggest that tungsten carbide vane-stage components will be required to establish the capability to withstand long-term exposure to the contaminated environment.

The present experimental fuel pump represents a significant step toward the development of flight hardware capable of operating at engine shaft speed. It meets the basic performance requirements of a main-engine fuel pump typically required on small, high-speed gas-turbine engines. In addition, it appears that a variable-displacement capability could be developed directly from the present hardware without altering the established high-speed capabilities.

TABLE OF CONTENTS

LIST OF ILLUSTRATIONS

LIST OF TABLES

LIST OF SYMBOLS

B	bearing pad width, in.
C	load variable, dimensionless
h_o	minimum film thickness, in.
R_t	tip radius, in.
R_{cr}	cam-ring radius, in.
U	tip surface speed, ips
W	tip load capacity, lb/in.
δ	effective crown, in.
μ	fluid viscosity, lb-sec/in.^{2}
CLA	Center-Line-Average

INTRODUCTION

The accessory systems on small gas-turbine engines presently represent from 25 to 35 percent of the installed weight, volume, and cost of the total engine. Significant improvements could be realized, however, by requiring the mechanically driven components of the accessory system to operate at or near engine speed. The development of such high-speed components would allow for a substantial reduction in the bulk and complexity of the required gear drive train.

A previous research program* conducted by Battelle's Columbus Laboratories for USAAVLABS under Contract No. DAAJ02-67-C-0037 resulted in the development of technology that makes feasible the operation of main-engine fuel pumps at speeds approaching engine shaft speed. Although the experimental hardware developed during that program was not capable of meeting all the realistic requirements of a gas-turbine fuel pump, it did demonstrate that a single-lobe vane pump could be successfully operated at speeds as high as 40,000 rpm without sacrificing pump durability.

The promising capabilities demonstrated by this experimental fuel pump resulted from the successful development of a hydrodynamically lubricated pivoting vane tip. This concept produces the low wear rates and power consumption normally associated with hydrodynamic lubrication in spite of vane-tip speeds in excess of 100 fps. The pivoting vane tip therefore provides the necessary features to operate a vane pump at turbine rotational speeds without major compromises in pump durability and efficiency.

The results of the previous program also revealed some operational deficiencies in the overall vane design at high fuel pressures. It was apparent that these deficiencies had to be eliminated before the basic performance characteristics of a main-engine fuel pump typically required on small, high-speed gas-turbine engines could be demonstrated. This report covers the continuing research effort which was directed toward the further development of the basic technologies previously established, with specific emphasis on the elimination of the high-pressure-performance deficiencies. The approach taken during the program was to apply the concepts generated to an experimental-fuel-pump design and to evaluate this pump at conditions predicted for future flight hardware. It should be pointed out, however, that the resulting experimental fuel pump is only a laboratory model which indicates one manner in which the concepts can be applied to produce a turbine-speed fuel pump. It does not represent a fully optimized design.

---

* Johnson, H.T., and Mitchell, R.K., ADVANCED HIGH-SPEED FUEL PUMPS FOR SMALL GAS-TURBINE ENGINES, Battelle Memorial Institute; USAAVLABS Technical Report 69-12, U.S. Army Aviation Materiel Laboratories, Fort Eustis, Virginia, April 1969, AD-688-972.

The design, fabrication, and performance evaluation of a single-lobe vane pump capable of operation at speeds up to 49,500 rpm and outlet pressures up to 900 psig while pumping JP-4 turbine fuel are described in this report. In addition, computer-generated design curves are presented which define the theoretical performance of the pivoting-vane-tip concept, and the application of this information to high-speed fuel pumps is described. Although the entire pump design is discussed in this report, the emphasis is on the areas of major change from the previous experimental hardware.

DISCUSSION OF RESEARCH

DESIGN OBJECTIVES AND APPROACH

The design phase of this program had the following fuel-pump performance objectives:

(a) Maximum speed: 50,000 rpm

(b) Fuel flow at 100 percent speed: 2,000 lb/hr

(c) Light-off fuel flow: 185 lb/hr at 6,000 rpm

(d) Design fuel pressure at 100 percent speed: 650 psig

(e) Light-off fuel pressure: 200 psig

(f) Maximum overpressure capability: 900 psig

(g) Fuel: MIL-F-5624 (JP-4)

The primary design objective was the establishment of high-speed capability with low-viscosity fluids such as JP-4. To achieve this capability without introducing additional complexities, it was determined that a fixed-displacement pump should be designed. It was also considered necessary, however, that the pump geometry be convertible to a variable-displacement configuration with no sacrifice of the high-speed capabilities. This consideration is important because of the overall fuel-system performance gains that could result from the use of a variable-displacement fuel pump. Particular emphasis was also placed on the contaminated-fuel resistance and the endurance capabilities of the individual pump components.

The techniques that proved successful during the previous research program were used as the foundation for the continuing development. The major design effort was directed toward achieving a vane configuration that would not exhibit structural weaknesses at high fuel pressures. It was necessary to eliminate the objectional undervane impact conditions exhibited by the earlier design without altering the undervane pressure-distribution requirements that had been experimentally established.

It was decided to minimize all efforts to optimize the design of the fuel-pump centrifugal charging stage and bearings. This was done because it was felt that these components could be more effectively optimized after the overall performance capabilities of the fuel pump had been experimentally defined.

FUEL-PUMP DESIGN

Discussion of Basic Concepts

The major difficulty associated with operating a vane pump at high rotational speeds is the resulting high vane-tip speed relative to the cam ring. Even for vane pumps with rotor diameters as small as 0.6 inch, the vane-tip speed exceeds 100 fps at 50,000 rpm. The use of conventional vane-tip boundary lubrication makes pump endurance questionable and produces high vane-tip drag forces which represent a considerable power loss at these tip surface speeds. These limitations are avoided through the use of the pivoting vane tip. The ability of the tip to support all radial-vane loading on a self-generated film of fluid was experimentally demonstrated by the earlier fuel-pump design at tip surface speeds up to 110 fps.

Because of these enccuraging results, no changes were made in the basic tip design for the latest fuel pump. However, significant changes were made in the design of the cam-ring profile which allow for a considerable improvement in the overall performance of the pivoting vane tip.

The factor which contributes most significantly to the load capacity of the tip is the relative surface profile between the bearing pad and the cam ring. For the fuel pump, a true radius is generated on the tip bearing pad which is slightly smaller than the cam-ring minimum radius of curvature. The maximum tip-bearing load capacity is obtained at this point of cam-ring minimum radius of curvature. At larger radii of curvature, the tip-bearing load capacity deteriorates,and the capacity obtained at the point of maximum radius of curvature generally establishes the maximum radial-vane loading that can be supported by the self-generated film of fluid without breakdown of this film. To optimize the tip-bearing design for all angular positions of a vane during the pumping cycle, it would be ideal if the cam-ring radius of curvature were constant. An eccentric-circular cam-ring profile was therefore chosen for the single-lobe pump design.

The eccentric-circular profile, with its constant radius of curvature, permits the maximum radial-vane loading to be approximately three times greater than the design loading for the earlier fuel pump. The increase is achieved because the maximum tip-bearing load capacity is available at all vane positions during the pumping cycle. Because no increase in bearing-pad width was required, the vane-assembly volume remained essentially constant.

The ability to design the fuel pump with increased radial-vane loads, as described above, is significant because it permits the use of higher density vane materials. The earlier fuel pump relied upon aluminum and carbon to obtain acceptable radial-vane loads at high rotational speeds. These low-density materials had inferior contamination resistance, however. Higher density sintered carbides, with their superior contamination resistance, can now be applied without compromising the overall pump design.

In addition to the above advantages, the circular cam profile allows the pump stroke to be selected without affecting the tip-load capacity. In the earlier fuel pump, the 0.020-inch stroke represented the maximum acceptable variation in the cam profile radius of curvature without severely compromising the tip-load capacity. With the circular profile, the stroke is dependent only on the eccentricity, and changes in the stroke do not cause variations in the cam profile. This allows the tip bearing to be designed without compromise and results in a pump design which can cover a much larger range of flow capacities without major modifications in the overall pump geometry. The 0.040-inch stroke chosen for the latest design permitted a 25-percent reduction in the rotor length in spite of a 50-percent increase in the pump theoretical capacity. To achieve this increase in capacity with the earlier design, a 50-percent increase in rotor length would have been required. The unbalanced rotor load carried by the journal bearings in a single-lobe vane pump would also have increased an equal amount. The circular profile therefore permits more flexibility in the overall design while providing improved pivoting vane-tip performance.

Because the pump stroke and capacity can be changed by varying the eccentricity of the circular cam ring, this design approach provides the feature required to obtain a variable-displacement configuration which does not affect the high-speed capabilities of the pivoting vane tip. Varying the eccentricity of a circular cam ring in a single-lobe vane pump is not unique. In fact, this is an established technique used in many industrial, variable-displacement hydraulic pumps. The resulting fixed-displacement fuel-pump design therefore exhibits reasonable potential for the evolution of a variable-displacement capability.

The fact that the eccentric-circular cam ring is easily adaptable to the pivoting-vane-tip concept and maximizes the high-speed properties of the tip is probably sufficient to justify its use. It should be pointed out, however, that the circular profile is also a simple configuration and minimizes the fabrication difficulties of the cam ring. A circular bore is easily generated even in the carbide materials required by the fuel pump contaminated fuel environment. The precision levels of cam-profile axial straightness required by the pivoting tip are also obtained by conventional manufacturing techniques.

The eccentric-circular cam-ring profile does require that the vane assembly stroke when subjected to a pressure differential on each lap space. This is a departure from the dwell-zone lap spaces used in the

earlier pump design and creates a potential vane-tip rotational-instability condition if the vane assembly is required to stroke radially outward under the pressure difference. By proper positioning of the inlet and outlet ports, however, the vane assembly can be made to stroke only radially inward when subjected to a pressure difference. Under these conditions, tip stability is not a problem. The porting configuration required is shown in Figure 1, a cross section of the fuel-pump rotor.

A major redesign of the vane assembly was required to eliminate the operational deficiencies associated with the earlier fuel-pump design. The objective was to produce an undervane hydrostatic-pressure distribution which would cause the vane assembly to track the cam profile without lifting from the cam surface, but would not produce excessive loading between the vane tip and the cam surface. Several vane configurations were investigated which met the basic requirements. Many were geometrically complicated, however, and some appeared sensitive to wear and contamination damage which might change the performance with time. The two-piece vane configuration shown in Figure 1 was chosen because its theoretical performance in the critical lap-space portions of the pumping cycle duplicated the experimentally proven conditions necessary to provide vane-tip stability at light-off without being sensitive to wear or contamination damage.

As noted in Figure 1, outlet pressure is applied continuously under a 0.030-inch-wide inner vane centered on the rotor-slot centerline. The remaining leading and trailing undervane areas are ported to the pressure ahead of and behind the vane assembly, through axially centered passages in the pump rotor on both sides of the vane slots. This provides the same vane radial balance on the lap spaces and the outlet port that was successful with the earlier fuel-pump design. On the inlet port sector, an additional load is produced that must be carried by the pivoting vane tip. This is due to the outlet pressure acting on the inner vane and the resulting radially outward differential pressure across the inner vane. This additional load could not have been carried by the tip with the two-radii cam-ring profile used in the earlier fuel-pump design. The increased radial-vane loading permitted by the circular profile again proved beneficial, however. The full optimization of the tip bearing allows the additional loading to be accepted without breakdown of the self-generated film of fluid.

A two-piece vane construction is not necessary to obtain the conditions noted above, for a T-shaped vane would be sufficient. The single-piece approach requires very precise rotor-slot and vane tolerancing, however, to minimize the undervane leakage losses when a vane assembly is located in the inlet port section of the pumping cycle. Therefore, to allow more conventional fabrication techniques to be used, the two-piece construction was adopted. This approach only requires that the inner vane/rotor slot clearance be precisely maintained. The relative location between the outer and inner slots becomes considerably less critical.

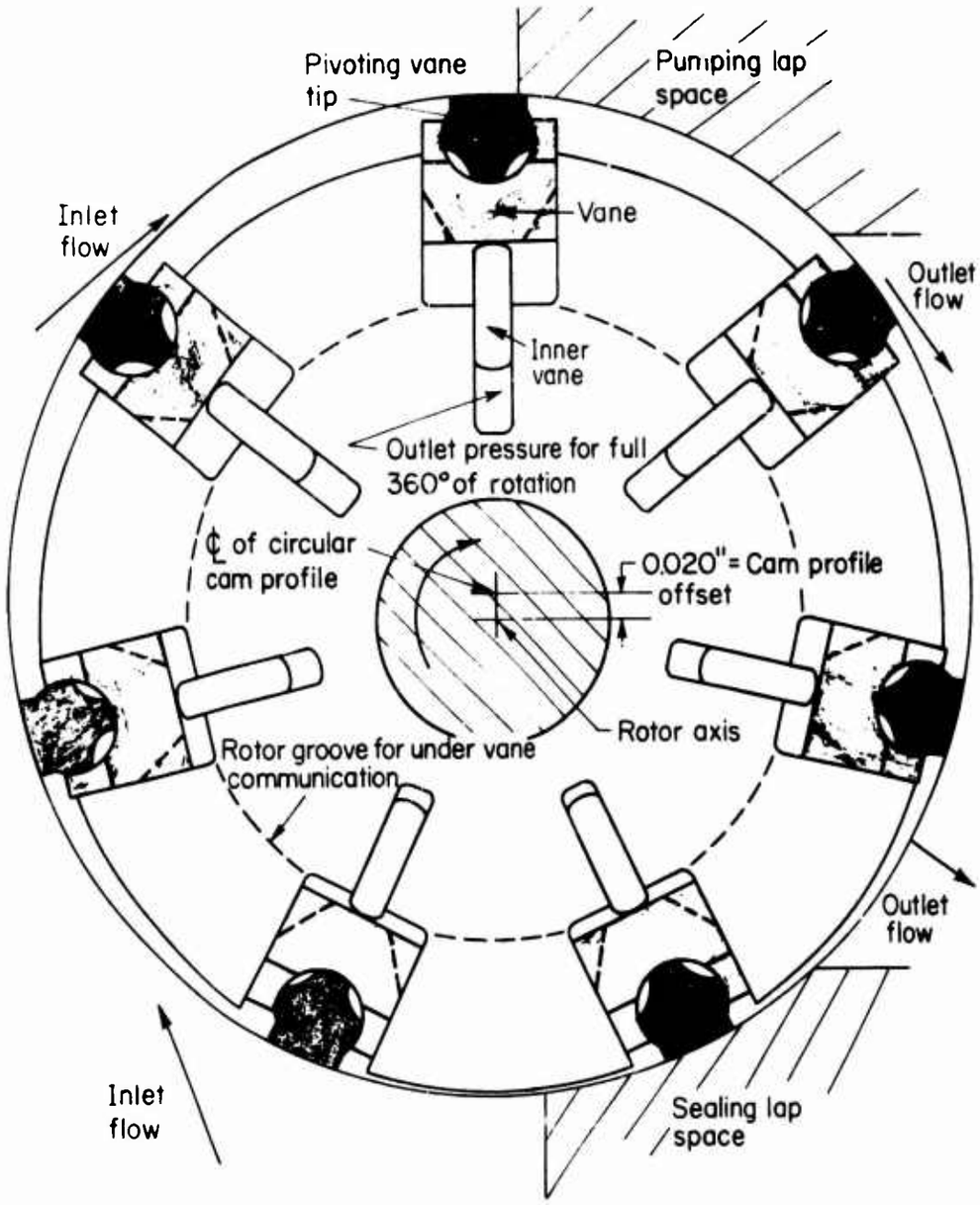

Figure 1. Fuel-Pump-Rotor Cross Section.

One potential disadvantage to the two-piece approach is the low vane-engagement ratio on the pumping lap space, where the vane assembly is required to stroke under a differential pressure. This risk was accepted, however, to minimize the hardware manufacturing costs. The contact between the inner vane and the outer vane ensures a positive seal between the leading and trailing undervane areas when the vane assembly is subjected to a differential pressure. Proper outward stroking of the inner vane on the inlet port is assured by the radially outward differential pressure across the inner vane.

A more quantitative discussion on the above subjects is found in Appendix II, where the theoretical performance of the pivoting tip as applied to high-speed vane pumps is described.

Description of Experimental Fuel Pump

The latest overall fuel-pump configuration shown in Figure 2 remains essentially identical to that used for the earlier pump hardware except for some minor design refinements in the individual components. It is a three-stage device incorporating an axial inducer in series with a centrifugal charging stage for the single-lobe vane stage. The fuel pump and its individual components have the following physical parameters:

(a) Pump theoretical capacity: 0.039 $in.^3$/rev

(b) Number of vanes: 7

(c) Vane stroke: 0.040 in.

(d) Rotor diameter: 0.740 in.

(e) Rotor length: 0.501 in.

(f) Cam-ring diameter: 0.790 in.

(g) Tip bearing-pad radius: 0.387 in.

(h) Tip bearing-pad width: 0.060 in.

(i) Outer vane width: 0.110 in.

(j) Inner vane width: 0.030 in.

(k) Centrifugal impeller diameter: 1.12 in.

(l) Journal bearing diameter: 0.700 in.

(m) Basic pump cartridge diameter: 2.4 in.

(n) Basic pump cartridge length: 5.5 in.

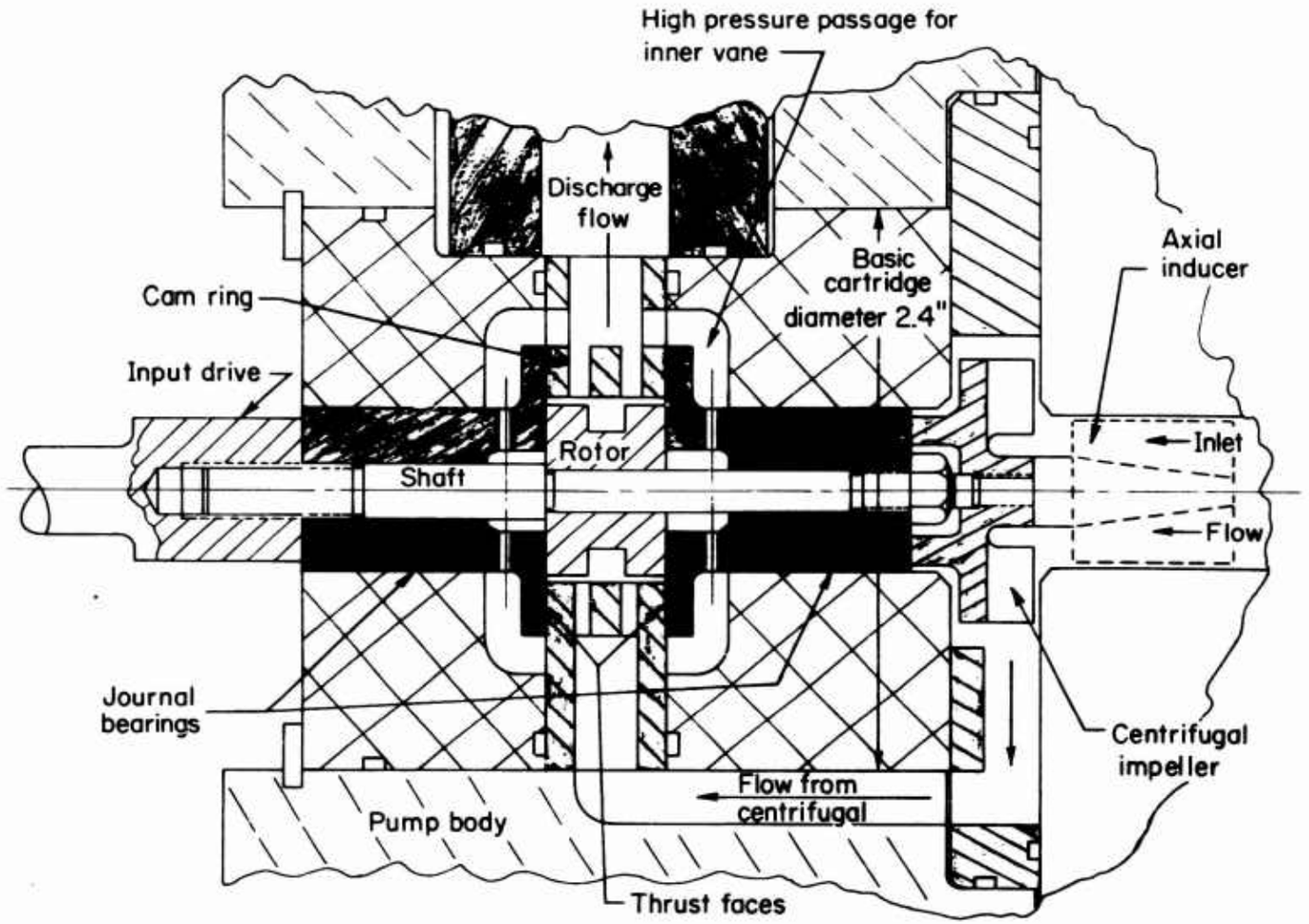

Figure 2. Fuel-Pump Assembly.

No changes have been made in the design of the centrifugal impeller or the axial inducer. The vane-stage design has been resized to provide for the 167-percent increase in the 100-percent speed flow requirements. The previous experimental hardware had a flow requirement of 750 lb/hr. Except for the basic changes in vane and cam-ring design, all other vane-stage modifications were made to allow for simplification of the fabrication procedures.

Figure 3 shows the basic pump cartridge and the various pump housing components. Two views of the rotor and a complete vane assembly are shown in Figures 4 and 5.

The centrifugal stage is an open-impeller (forced vortex) pump. The impeller has straight radial blades and is enclosed by a circular housing which is concentric to the impeller. This impeller design proved capable of meeting the high-head and low-flow requirements of the fuel pump during the earlier program. The recovery of the velocity head developed by the impeller was poor owing to improper diffuser design, and the resulting efficiency of the centrifugal stage was lower than normally expected. In the latest design, this condition was improved by reducing the clearance between the impeller and the housing and incorporating a simple discharge nozzle located tangential to the periphery of the housing. Owing to this change, the percentage of dynamic head recovered has increased from 20 to 50 percent. The final design develops a 260-psig head at 40,000 rpm and has the flat head-flow curve which is characteristic of this type of pump.

Both the axial inducer and the centrifugal impeller are cantilevered on the vane-pump rotor shaft opposite the drive end. The open-impeller design minimizes the axial-thrust loads and permits the use of compact hydrodynamic thrust bearings. The concentric housing, in which the forced vortex is formed, produces a uniform radial pressure field, and no radially unbalanced forces are generated. The open-impeller design and the concentric housing bore are extremely simple and lend themselves to simplified fabrication methods. The radial blades on the impeller are also not subjected to any appreciable bending by the high centrifugal forces created by turbine rotational speeds.

The number of vanes in the vane stage has been increased from six to seven. The choice of an odd number of vanes was made to minimize the potential pump flow ripple. To achieve this increase, it was necessary to increase the rotor diameter 25 percent. The larger rotor diameter permitted the use of a two-piece rotor and shaft construction which simplifies the fabrication of these components. The rotor diameter was chosen so that it permitted these changes and still was consistent with reasonable tip velocities, fluid flow losses, and the charging pressure available to accelerate the fluid to vane-tip speed. The increased rotor diameter, in combination with the stroke increase and rotor-length decrease, actually resulted in a decrease in the unbalanced side loading carried by the journal bearings.

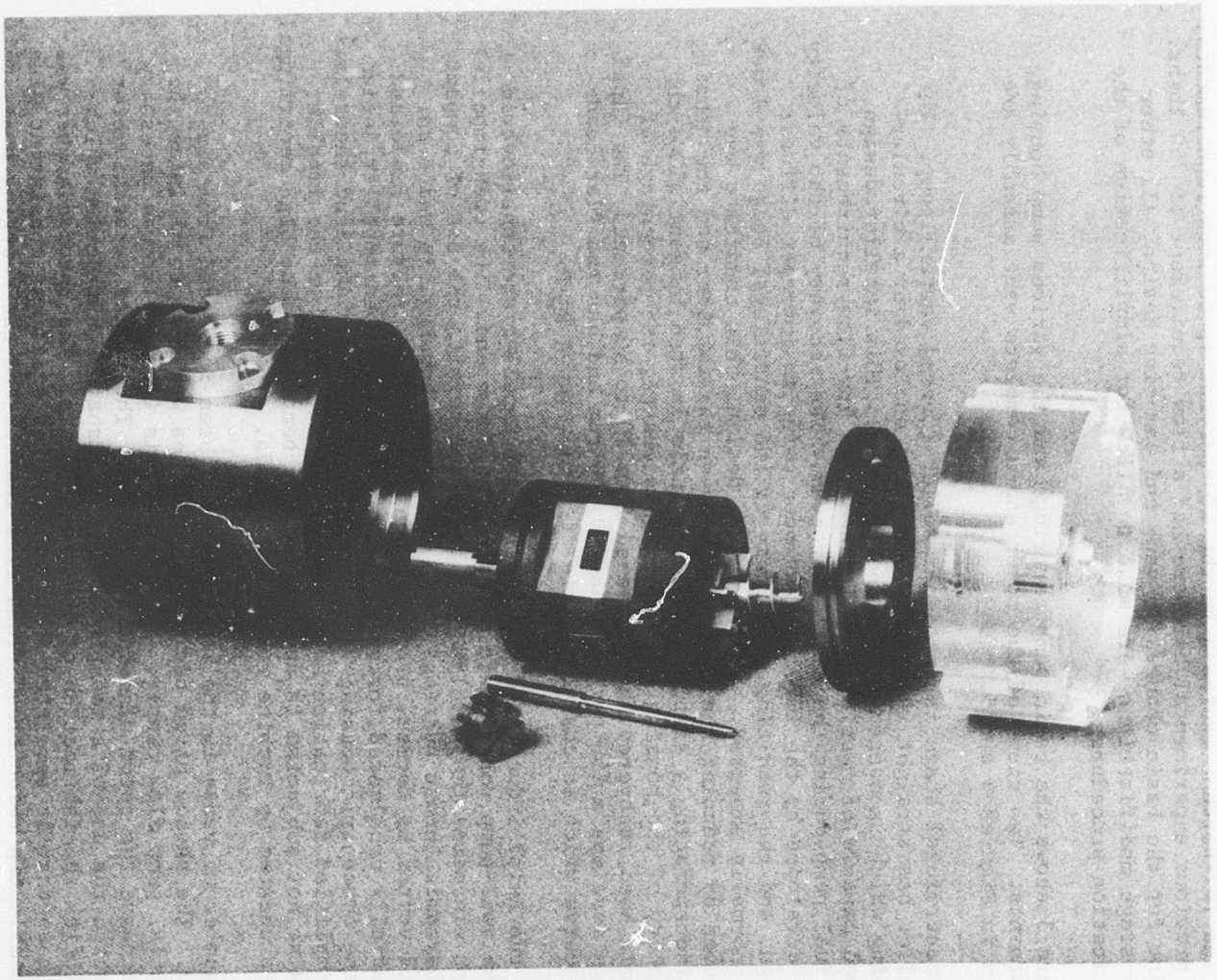

Figure 3. Fuel-Pump Components.

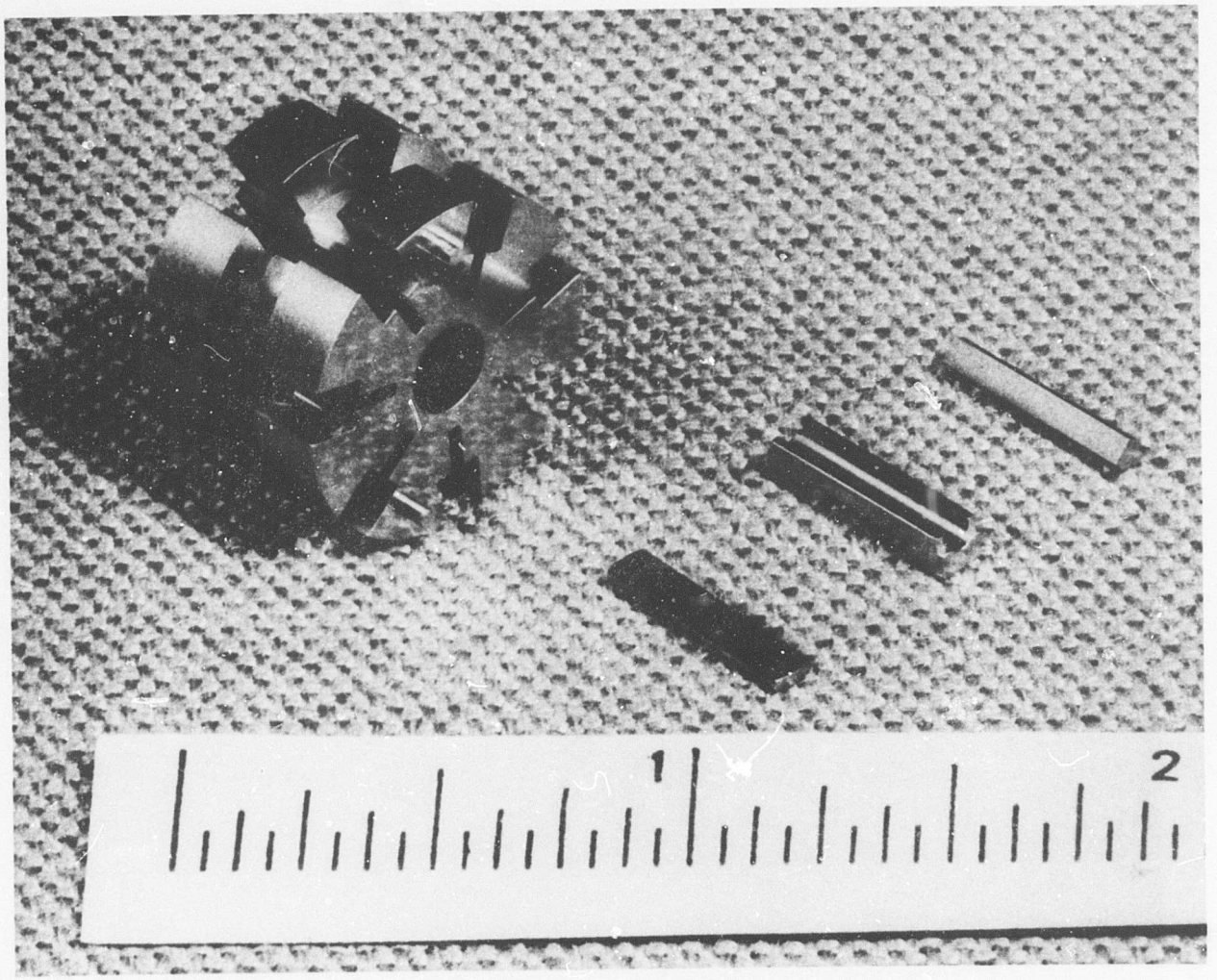

Figure 4. Fuel-Pump Rotor and Vane Components.

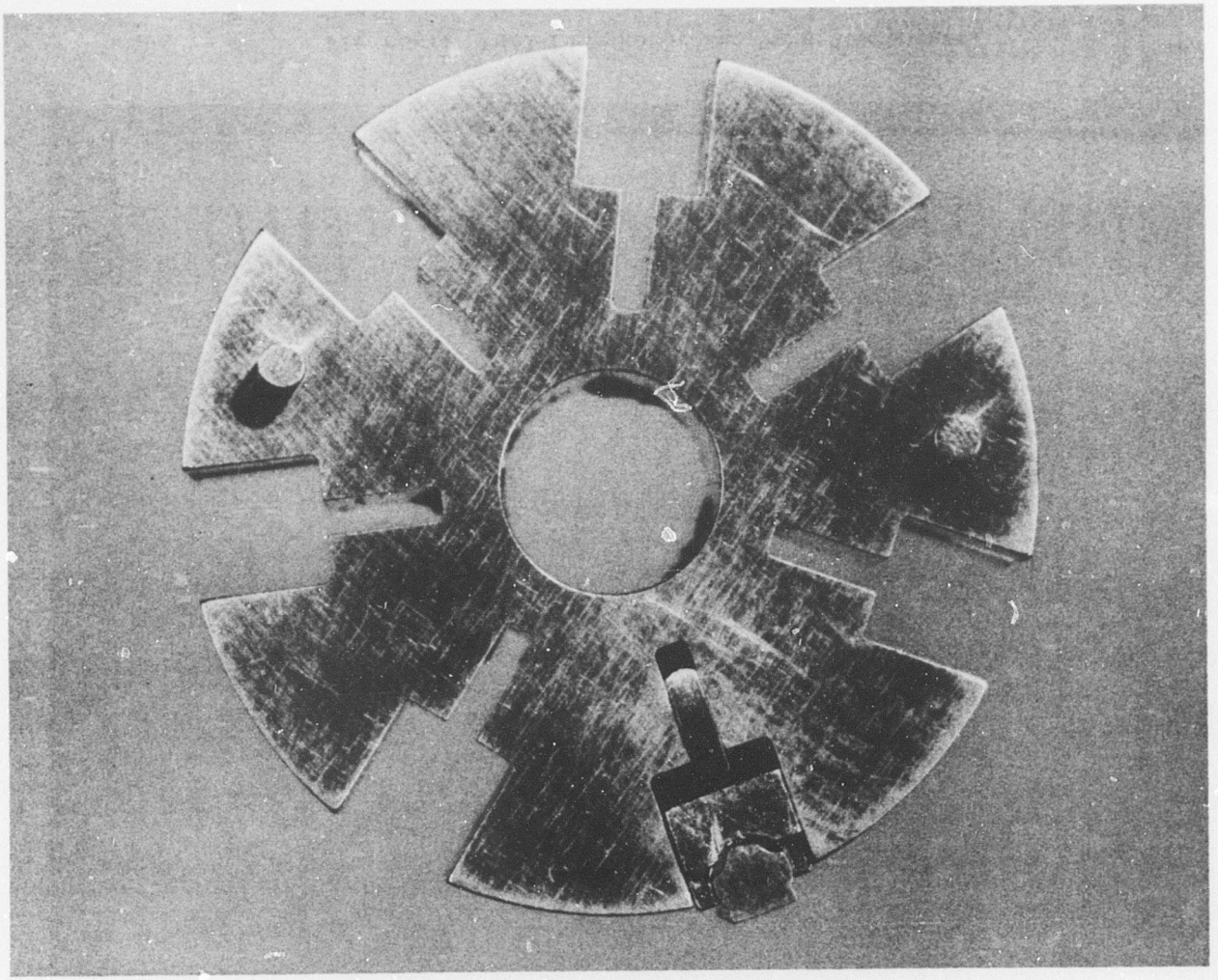

Figure 5. End View of Fuel-Pump Rotor and Assembled Vane.

The vane-stage design still incorporates the rotating end plates which also serve as thrust bearings to stabilize the axial rotor motion at high speed and to carry any thrust load applied to the rotor shaft. These fuel-lubricated stepped-land thrust bearings use the sides of the cam ring as a thrust surface, as indicated in Figure 2. A pair of hydrodynamic journal bearings support the radial hydrostatic load produced by the unbalanced single-lobe configuration. These bearings are also fuel-lubricated with high-pressure fuel from the outlet port. The journal bearing diameter has been made smaller than the cam-ring bore to permit the sleeve diameters to be line-bored as an assembly with the cam ring. The outside diameter of the sleeve bearings and the cam ring forms the basic envelope for the pump cartridge. The location of the axis of rotor rotation relative to the cam-ring bore is properly established by doweling the sleeve bearings and cam ring together.

All porting to and from the vane-pump stage is radial through the cam ring. As noted in Figure 1, the inlet port covers the entire 180 degrees while a vane is stroking outward. The outlet port covers the center 90 degrees of the inward-stroking vane cycle. The widths of the lap spaces are such that they are approximately 0.030 inch shorter than the circumferential distances between the leading and trailing edges of two successive vane tips. Outlet pressure from the outlet port is communicated continuously under all inner vanes through radial holes in both journal bearings.

During the selection of the pump-component materials, the major emphasis was placed on obtaining contamination-resistance and high-speed-endurance capabilities. The component materials used during the pump-endurance and contaminated-fuel evaluations are listed in Table I for the major pump components. The materials selected represent a compromise between the pump design, fabrication, and contamination resistance requirements. The approach taken during the program was to initially choose materials which provided minimum fabrication costs while sacrificing endurance capabilities until the basic performance of the pump had been determined and qualified. This approach was used particularly with the vane assembly components, where design changes during the program were to be expected during the early performance evaluations. Once the design performance was qualified, however, more durable materials were selected.

The materials selected for the vane assembly components are the most critical since they not only affect durability and cost, but their density also establishes the level of radial vane loading to be accepted by the pivoting tip. For optimum contamination resistance, the tungsten carbide cermets are the most logical choice, but their very high density (S.G. = 15) produces vane loads in excess of the maximum anticipated tip load capacity based on the previous experimental results. Experience gained during the program, however, makes their future use much more feasible. Titanium carbide cermets (S.G. = 6), such as Ferro-Tic C and the molybdenum-bearing cermet used for the outer vane, represent a reasonable compromise. Early outer vanes were electroless nickel-plated

TABLE I. COMPONENT MATERIALS LIST

Component	Material
Rotor	D-2 tool steel, hardened and double tempered to 59/61 Rc
Cam Ring	Ferro-Tic C, hardened to 68/71 Rc
Outer Vane	Molybdenum-bearing titanium carbide
Inner Vane	Ferro-Tic C, hardened to 68/71 Rc
Vane Tip	Ferro-Tic C, hardened to 68/71 Rc
Journal Bearing	SAE No. 67 leaded bronze
Journal and Thrust Bearings	Ferro-Tic C, hardened to 68/71 Rc

aluminum, but these were discarded once the performance results indicated that the basic vane configuration had eliminated the problems previously experienced with the previous fuel pump and had the proper performance characteristics to freeze the design.

The use of Ferro-Tic C was continued for the cam ring and the journal and thrust bearings. It has the necessary endurance capabilities and minimized fabrication costs for the experimental pump. Since material density has no effect on the performance of these components, tungsten carbide cermets should be considered for future use to improve the contamination resistance. The use of D-2 tool steel for the rotor provides reasonable abrasive-wear resistance without introducing fabrication complexities. Directly hardened high-carbon, high-chromium tool steels such as D-2 have increased wear resistance because of the presence of hard chromium carbide particles produced during the heat treatment.

Fabrication of Experimental Fuel Pump

During the design phase of the program, considerable emphasis was placed on component configurations that not only met the pump performance requirements but also lent themselves to production manufacturing techniques. The experimental fuel pump is only a "bar stock" prototype, however, and some compromises to the above approach had to be made to minimize program fabrication costs. This is particularly evident in the area of component material selection. Tungsten carbide cermets would be a more appropriate choice for the cam ring and journal bearings in production quantities where they could be more economically preformed prior to the final grinding operations. For the experimental pump, the tooling required for preforming was too expensive, and a machinable carbide such as Ferro-Tic C was chosen. Such materials allow the wear-resistant qualities to be obtained by heat treatment after rough machining to shape from stock blanks.

In general, the fuel-pump design requires the use of precision machining techniques to meet the demands of high rotational speeds. The pivoting vane tip and the journal and thrust bearings require close control of the component tolerances if the high relative surface speeds are to be achieved at the very small operating clearances required. As a result, tolerances for straightness, parallelism, concentricity, absolute dimensions, etc., on components which operate with these clearances are in the 0.0001-inch order of magnitude. It may be possible to relax these tolerances, however, once more experimental high-speed experience is acquired. The use of hard, wear-resistant materials to survive the contaminated-fuel environment also requires final grinding and lapping operations in the hardened state to obtain the precise tolerances. The component forms are generally simple, however, and the tolerances can be maintained at reasonable costs.

The potentially most difficult components to manufacture are the pivoting vane tip and the outer vane, particularly from carbide. The fabrication

techniques used for the tip proved quite successful, however. The tip bearing-pad radius was generated in a fixture which allowed it to be ground in a manner similar to grinding a complete diameter. Final inspection was performed in the fixture, and later inspections using a Talysurf surface measuring instrument verified that the pad profile was correct within 20 microinches. The socket diameters on the tip and the outer vane socket proved difficult to manufacture and in both cases were form ground. The shortened axial length of the vane pump helped to minimize these difficulties, but simpler configurations should be considered in the socket area. The socket design shown in Figure 1 has a vane socket diameter which wraps around the tip socket diameter a sufficient amount to prohibit radial separation of the tip from the outer vane during startup. The amount that it envelopes the tip has to be minimized, however, to insure that the tip can rotate properly within the angular range required during the pumping cycle. This type of design requires that very close tolerance be maintained to insure that both conditions are met. Experience gained during the program on the operation of pivoting tips suggests, however, that other approaches to this problem are feasible which would permit a considerable relaxation in the component tolerances.

Although emphasis was placed on simple component configurations, the approach to component tolerances for the experimental fuel pump actually made fabrication more difficult, particularly for the rotor and the vane assemblies. Because of the experimental nature of the program, close control of the tolerances was maintained to insure that deviations from the theoretical ideal conditions would not cloud the understanding of the pump performance results. It was felt that a more realistic relaxation of the tolerances could be made after the design was qualified and its performance characteristics more thoroughly understood. Similarly, close control of the rotor, rotor shaft, and journal bearing assembly was maintained to insure repeatable pump assembly conditions and to allow any potential design modifications to be incorporated interchangeably with the original components. The line-to-line fit between the rotor shaft and the rotor and journal bearings and the tightly controlled concentricity between diameters on these components are consistent with the above approach. They insure that the theoretically ideal conditions are actually achieved at a point in the pump development where the actual limits based on pump performance have yet to be determined.

All pump components except the centrifugal impeller and the axial inducer were fabricated by the Speedring Systems Division of Schiller Industries, Inc., Warren, Michigan. The impeller and the axial inducer from the earlier fuel pump were again used in the latest pump. All tooling was designed and supplied by Speedring, and the fabrication techniques used reflect the prototype level of production quantities required to produce one complete fuel pump plus sufficient spare hardware to minimize program delays when component failures were encountered. The fabrication costs for one pump assembly were reasonable (on the order of $10,000), considering the present experimental level of the pump development.

During discussions with Speedring manufacturing representatives concerning the pump's potential for production manufacture, it was indicated that the present design had no characteristics which would be considered impractical or unusually difficult to manufacture in production quantities. A complete manufacturing cost study has not been made, however, since the dimensional limits required to insure reliable pump performance have not been determined. In addition, this task was not part of the program objectives.

FUEL-PUMP PERFORMANCE EVALUATION

Basic Performance Results

The experimental fuel pump has been subjected to a series of performance tests designed to evaluate its abilities to meet the original performance objectives while pumping clean, room-temperature JP-4 with the inlet pressure essentially atmospheric. The test program was designed not only to obtain the overall pump characteristics, but also to determine the performance of the individual components and their effect on the overall performance. The latter data are required to completely understand the overall results and help to point out the trade-offs required to achieve high-speed accessory components such as the main-engine fuel pump.

The initial objective of the test program was to qualify the fuel pump over a 6000- to 25,000-rpm speed range, with a maximum outlet pressure of 500 psig to be achieved at 25,000 rpm (400-psi vane-stage differential pressure). During this phase, the majority of the necessary design modifications were made. During the next phase, the pump was evaluated up to 40,000-rpm, 650-psig outlet pressure conditions. The speed was increased in 5,000-rpm increments, and a maximum vane-stage differential pressure of 400 psi was maintained at each speed. Further higher speed testing was accomplished with a constant outlet pressure of 650 psig and with the speed increased in increments of 2500 rpm up to 49,500 rpm. In addition to the above tests which were run on the complete fuel-pump assembly, the performance of the centrifugal stage plus the pump bearings was obtained up to 45,000 rpm by removing the vane assemblies from the vane-stage rotor. This information, plus the performance characteristics of the impeller determined in the earlier program, permits a component power-distribution analysis to be made.

The overall performance results obtained for the final pump configuration are given in Table II. The experimental flow-performance curves for various pump speeds are shown in Figure 6. The maximum speed achieved during the evaluation was 49,500 rpm, with an outlet pressure of 680 psig. Further higher speed evaluation was terminated because of the power limits of the flat-belt speed-increaser drive. Belt slippage at speeds exceeding 45,000 rpm led to the decision to make 40,000 rpm the 100-percent design speed for the 200-hour endurance test. On the basis of this decision, 40,000 rpm was also chosen as the point to qualify the pump at the 900-psig overpressure condition. It should be pointed out, however, that there was no evidence during the performance evaluation

TABLE II. OVERALL PERFORMANCE RESULTS

RPM	Outlet Pressure (psig)	Centrifugal Head (psig)	JP-4 Flow Rate at Pressure (lb/hr)	Volumetric Efficiency (%)	Overall Efficiency (%)	Input Power (hp)
6,000	200	6.5	225	59	52	0.14
15,000	330	35	770	80	53	0.73
25,000	500	104	1330	83	46	2.2
30,000	545	148	1630	86	43	3.1
35,000	600	200	1920	87	41	4.4
40,000	650	258	2220	88	38	5.9
40,000	900*	262	2040	80	42	6.8
42,500	650	285	2360	88	36	6.6
45,000	650	320	2520	89	34	7.5
47,500	650	355	2680	89	33	8.3
49,000	670	370	2770	89	32	9.1

* Overpressure condition.

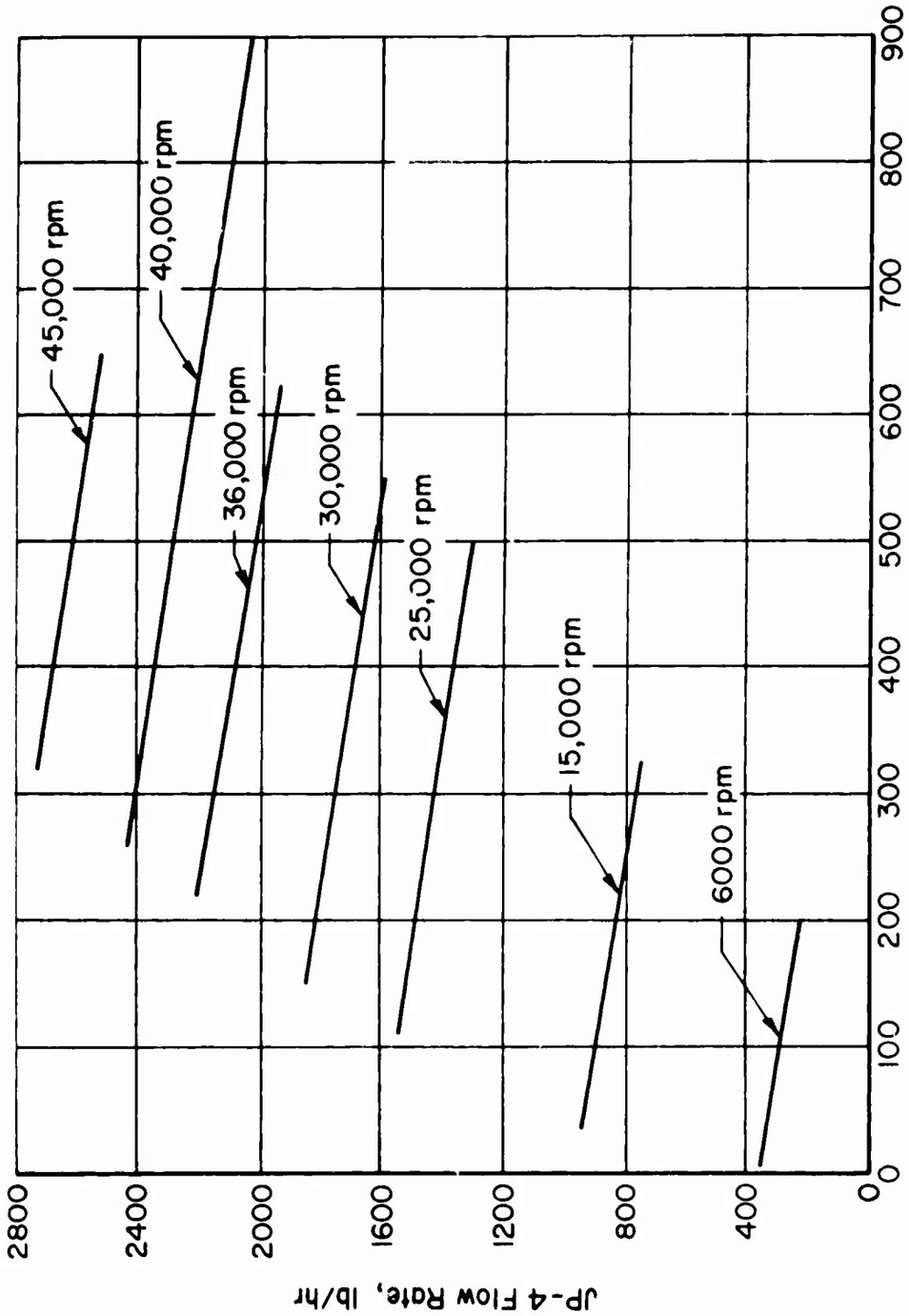

Figure 6. Fuel-Pump Flow Performance Curves.

to indicate that the maximum pump speed is limited to 49,500 rpm. These results were very encouraging because the pivoting vane tips were required to support a maximum load of 122 lb/in. with a relative surface speed of 180 fps at the 49,500-rpm test conditions. This far exceeds any previous tip speeds and loads using JP-4 as a lubricant. Inspection of the tip bearing pads and the cam-ring bore surface with a Talysurf surface measuring instrument revealed no evidence of contact.

Two major design problems were encountered during the early performance tests at speeds up to 25,000 rpm. The first of these was encountered during the first pressure tests at 25,000 rpm, when a breakdown of the vane-tip hydrodynamic films occurred as the outlet pressure was increased to 375 psig. A subsequent analysis revealed a design error in the location of the inlet and outlet port intersections with the cam contour. The cam ring was originally designed to provide a zero underlap condition with respect to the vanes on both the pumping and sealing lap spaces. With zero underlap, there is an instant on both lap spaces in which the fluid between the vanes is sealed from both the inlet and outlet ports, because the lap space peripheral length is equal to the distance between the trailing and leading edges of a pair of vane tips. This condition is satisfactory if a vane is not required to stroke on a lap space. However, with the eccentric-circular cam contour, this is not the case. For example, on the pumping lap space the leading vane is stroking inward, and as a result a flow rate is established from the volume between the vanes to the inlet port until the volume is exposed to outlet pressure. A theoretically infinite pressure is developed between the vanes at the instant the flow is sealed from both ports. This condition would have occurred at all outlet pressures, except that the inner vanes acted as relief valves for low outlet pressure conditions. As the outlet pressure was increased, a higher pressure had to be developed between the vanes before the inner vanes would separate and provide a flow path to the ports.

To correct this condition, the inlet-port intersections with the cam contour were moved 0.030 inch to provide 4.5 degrees of underlap on both lap spaces. Theoretical calculations indicated that this amount of underlap would insure that the pressure buildup in the lap-space volumes would not exceed approximately 200 psi at 50,000 rpm.

It was originally felt that the very high pressures produced in the lap-space volumes increased the magnitude of the vane drag to the point that it overloaded the vane tip bearing and produced tip hydrodynamic-film breakdown. In fact, the changes in the port timing resulted in the successful operation of the pump at 25,000 rpm and 500 psig with no evidence of the above problem. This therefore tended to verify that the timing was the sole cause. The 500-psig condition proved to be the approximate threshold at which tip hydrodynamic-film breakdown would again occur, however, for subsequent operation at this condition resulted in tip failures very similar to those previously occurring at lower pressure.

The continuing tip failures led to the decision to conduct further experiments with the pivoting tips to determine their load-carrying capabilities under known loads. This was accomplished by operating the pump with a single vane and vane tip and without the inner vane. The only vane-tip loading was caused by the acceleration loads produced by the rotating mass. The effects of a pressure differential and the resulting vane drag were eliminated. The objective of this experiment was to operate a tip at a speed which would produce a theoretical tip film thickness equal to that anticipated for the 25,000-rpm and 500-psig conditions. This 31-microinch film thickness was achieved at 42,500 rpm with a Ferro-Tic C vane tip and a titanium carbide vane.

Two different tips were operated successfully under the above conditions. An inspection of the tip bearing-pad surfaces and the cam-ring bore surface revealed no evidence of contact or film breakdown. The tip surface speed of 154 fps and loading of 75 lb/in. far exceeded any previous conditions with JP-4 as the lubricant.

The successful results of the above experiments plus a review of all previous pump-performance data produced the conclusion that all the results were inconsistent unless it was assumed that the straightness of the cam-ring bore changed when a differential pressure was applied across the vane stage. An examination of the structural characteristics of the cam ring showed that this assumption was correct. The long, axially unsupported section of the inlet-port area had insufficient stiffness. Consequently, deviations were produced in the straightness of the cam-ring bore in the inlet port when the vane stage was subjected to a differential pressure. This allowed the outer edges of the ports to deflect radially (approximately 30 microinches) toward the tip bearing pads, causing tip contact. Deflections in other areas of the inlet port were such as to increase the operating film thickness. This reduced the available load support from these areas of the cam ring, further aggravating the problem. Axial supports were placed in the inlet port at the cam-ring outside diameter which eliminated the cam-ring deflections. No further difficulties with vane-tip operation were encountered after this modification.

The elimination of the cam-ring axial deflection also produced a significant decrease in the pump leakage rate. It was apparent that the axial deflection produced a large clearance at the thrust bearing surface, allowing considerable leakage of high-pressure fluid into the inlet-port area. Figure 7 provides a direct comparison of the flow rate before and after the installation of the cam-ring supports at the 25,000-rpm evaluation conditions.

It is felt that the cam-ring deflection was the major cause of the early difficulties encountered with the pivoting vane tip. The effect of the improper port timing should not be discounted, however. The fact that the inner vanes acted as relief valves probably made the effect less pronounced. The use of vane underlap is required for this

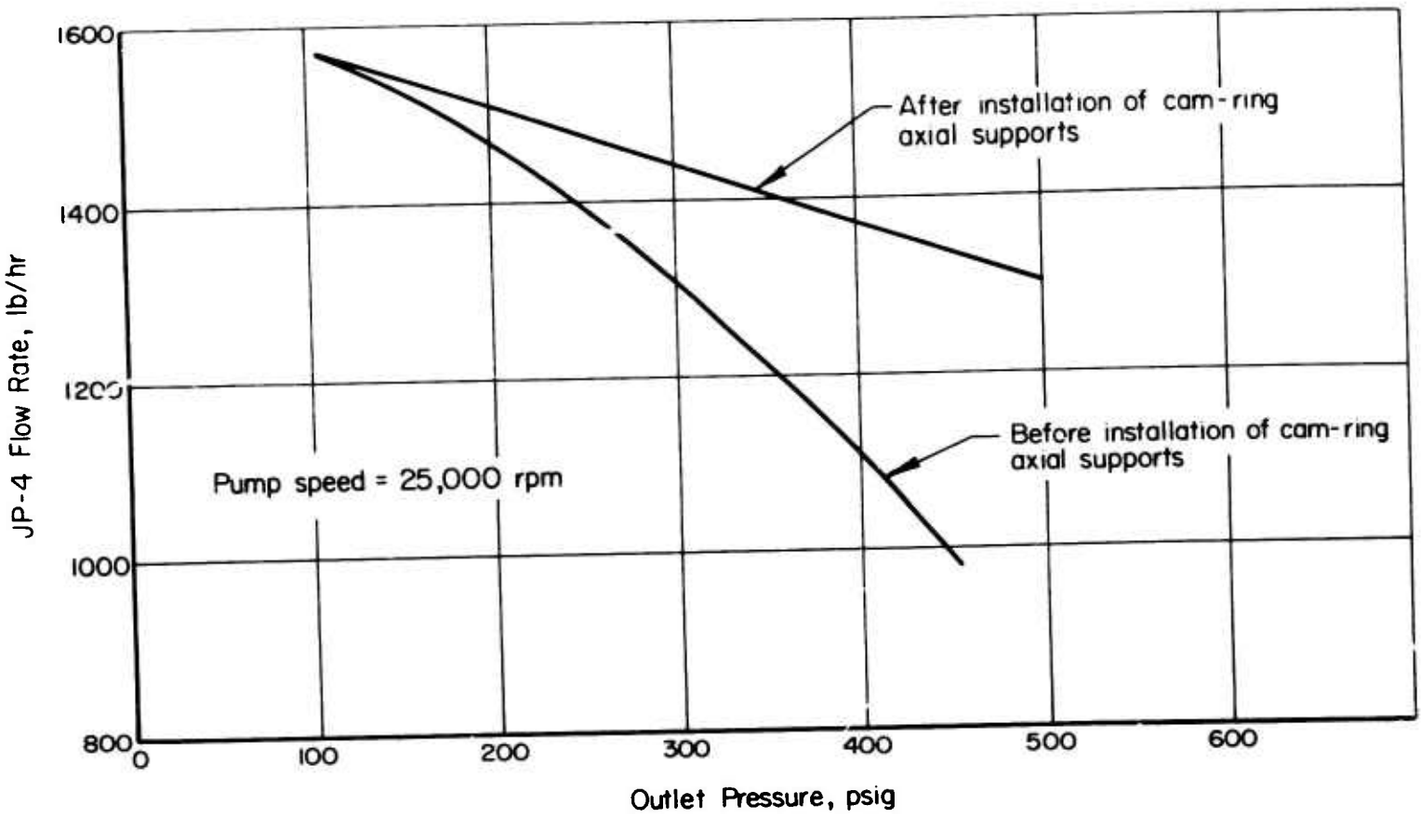

Figure 7. Comparison of Flow Rates Before and After the Installation of the Cam-Ring Axial Supports.

pump design and is particularly important at high rotational speeds. The exact effect of variations in the underlap at different speeds was not evaluated further, however, since the chosen 4.5 degrees of underlap appeared sufficient when combined with the cam-ring axial supports. It should also be noted that this amount of underlap does not appear to significantly affect the pump leakage rate. The leakage rate is essentially at the level anticipated during the design phase and results in a light-off flow rate of 225 lb/hr at 200 psig, which exceeds the required 185 lb/hr.

A high-response pressure transducer was installed in both the pump outlet and the interstage volume to determine the pressure-pulsation characteristics of the pump. In the outlet port, a ripple magnitude of 6 psi peak to peak with a frequency of 14 times rotor rpm was obtained for the 40,000-rpm, 650-psig conditions. At lower speeds, the outlet ripple was of the same order of magnitude with a frequency of either 7 or 14 times rotor rpm. This low level of outlet-pressure pulsation represents a significant improvement over the results obtained with the earlier experimental fuel pump where pressure pulsations up to 230 psi peak to peak were noted.

A different condition existed in the interstage volume. A constant-frequency (14,000 cycles/second) signal was noted at all speeds. The magnitude of this signal was speed sensitive and increased rapidly as the speed approached 41,000 rpm, where the ripple magnitude reached a maximum of 162 psi peak to peak. At higher speeds, the magnitude decreased. It was determined that the 14-kc frequency noted is the resonant frequency of the interstage volume. The condition of resonance occurs at approximately 41,000 rpm. The same 14-kc signal was also noted in the interstage volume when just the centrifugal stage was assembled and operated across the pump speed range. The magnitude was much lower during the centrifugal test, however, for the vane pulsations were not available to provide the disturbing force. Theoretical estimates also indicate that the resonant frequency of the interstage volume is approximately 14 kc.

The interstage volume pressure pulsations do not appear to have a major effect on the pump performance over the speed and pressure ranges evaluated. This is probably due to the fact that the centrifugal charging pressure is conservative and the vane-stage inlet pressure never drops low enough to produce filling problems. No attempts were made to change the interstage volume resonant frequency, but tuning of this volume would probably be required during an optimization of the pump design where the centrifugal head would be minimized to require the more efficient vane stage to supply a greater percentage of the higher speed pump head.

In conjunction with the noted pulsation in the interstage volume, a small amount of cavitation erosion was noted on the end plates of the vane stage. Although it is possible that this may be related to the

inlet pulsations, it is felt that the basic cause is just localized cavitation due to obstructions in the inlet flow. Prior to installation of the axial supports in the cam-ring inlet, no erosion was noted. The supports represent an obstruction, however, and may cause locally high velocities and cavitation in the inlet port. The bubbles created are probably carried into the vane stage,where they centrifuge to the bottom of the outer vane slots and collapse against the end plates when subjected to outlet pressure. Additional undervane flow passages were placed at the ends of one rotor in an attempt to minimize the cavitation damage, but no attempts were made to attack the cause since it had little effect on the pump performance or endurance capabilities. The flow passages eliminated the condition in which the bubbles were directed perpendicular to the end plates,where they cause erosion upon collapsing. The additional passage did not eliminate the damage completely, however. The cavitation bubble collapse occurred in the added flow passages, but it produced a much lower rate of erosion.

Endurance Evaluation Results

The operating conditions and the duration at each condition for the 200-hour endurance test are listed in Table III. These are comparable to typical flight conditions for a military-helicopter gas turbine. The 200-hour test was divided into two segments. A preliminary, 24-hour evaluation was conducted prior to attempting pump speeds above 40,000 rpm. The 24-hour period was separated into four 6-hour segments at 25,000, 30,000, 35,000, and 40,000 rpm, respectively. The decision to perform a preliminary endurance evaluation was made in order to obtain the maximum amount of wear data before proceeding with the higher risk conditions.

The remaining 176 hours of evaluation was conducted after the pump was evaluated at the maximum speed of 49,500 rpm and the overpressure test of 900 psig at 40,000 rpm. The total time was broken into 50 cycles, 3-1/2 hours in duration. Each cycle started at 26,000 rpm, 510 psig and proceeded toward 40,000 rpm, 650 psig, with intermediate periods at 30,000, 32,000 and 36,000 rpm. As previously noted, 40,000 rpm was chosen as the 100-percent speed point. The design outlet pressure of 650 psig at this speed produces approximately a 400-psi differential pressure across the vane stage. This 400-psi differential pressure was maintained at all lower speeds to obtain the maximum amount of operation at this condition. This represents an accelerated test, since typical flight conditions would probably permit lower outlet pressures at these speeds than noted in Table III.

During the final performance and endurance evaluations, one set of pump components was successfully operated for a total of 225 hours over a speed range from 6,000 to 49,500 rpm. At no time during this period was there any evidence of fuel-pump performance degradation. The pump performance parameters were continuously monitored during this period. A complete inspection of all pump components was made

TABLE III. ENDURANCE SCHEDULE

Speed (rpm)	Outlet Pressure (psig)	Time at Conditions (hr)	Percentage of Total Time
25,000	500	6	3
26,000	510	8	4
30,000	550	24	12
32,000	570	44	22
35,000	600	6	3
36,000	620	79	39.5
40,000	650	33	16.5
	Totals	200	100

prior to initiating the 50-cycle endurance test and after 10, 20, 39, and 50 cycles. No unusual or excessive wear was observed on any of the individual components. Both the tip bearing pads and the cam-ring bore surface were inspected using a Talysurf surface measuring instrument. The original 0.6-microinch CLA (Center-Line-Average) surface finish on the bore and the 6.0-microinch CLA surface finish on the pads remained unchanged in spite of the fact that the surfaces were measured at 50,000X and 10,000X magnification, respectively. They bore no evidence of contact or wear throughout the entire endurance evaluations, where the maximum tip surface speeds ranged from 90 to 144 fps.

The only individual component replaced during the entire 225-hour period was the vane-stage rotor. The rotor was replaced so that the effects of the additional undervane porting in the rotor could be evaluated. An inspection of the rotor revealed no evidence of excessive wear, and it still met the original manufacturing requirements. The modified rotor was used during the final 30 cycles (105 hours) of the endurance evaluation.

The cavitation damage on the end plates was minor and did not affect the performance of the pump during the endurance evaluation. The worst-case area was a small pit located at the bottom of each outer vane slot. It was approximately 0.025 inch in diameter with a maximum depth of 0.003 inch.

The only other measurable wear noted during the endurance evaluation was confined to the trailing edges of the outer vanes and the inner vanes. This wear represents an average weight loss of 1.0 milligram for the outer vanes (nominal weight = 0.330 gram) and 0.3 milligram for the inner vanes (nominal weight = 0.154 gram). The wear zone was located at the contact point of the outer and inner vanes with the outer edge of their respective slots when they are in the maximum extended position on the pumping lap space. The low vane-engagement ratio permitted the vanes to tilt slightly, producing an axial line contact zone while the vanes are stroking inward on the pumping lap space under a differential pressure. On the outer vane, the wear zone is a 0.035-vane-wide area along the axial length of the vane with a maximum average depth of 270 microinches after 225 hours of operation. On the inner vane, the wear pattern is a 0.025-inch-wide area along the axial length with a maximum average depth of 290 microinches after 225 hours of operation. This wear did not affect the pump performance, and the wear rates were decreasing with increased operating time. It is felt that this condition represents a "wear-in" period as an area contact zone is established. The "wear-in" period is of extended duration because of the low wear rates of the carbide materials used.

The wear in the vane-tip socket area was negligible. The total average vane-tip weight loss was only 0.1 milligram (nominal weight = 0.193 gram). Repeated Talysurf inspections on the vane-tip bearing-pad radii

at 2,000X magnification revealed no evidence of change during the endurance evaluation. The pump journal and thrust bearings also survived the endurance evaluation with no measurable wear or evidence of breakdown of their respective hydrodynamic films.

Contaminated-Fuel Evaluation Results

The experimental fuel pump was subjected to a series of contaminated-fuel tests designed to determine the mechanical-erosion resistance of the fuel pump and the susceptibility of the basic design concepts to the contaminated environment. The same pump hardware that had completed 200 hours of endurance testing was used for the contamination evaluations. It was felt that the performance characteristics of the fuel pump could be more realistically defined if the same hardware was used during both the endurance and contamination evaluations. In addition, the hardware met the original manufacturing print requirements at the completion of the 200 hours.

During the first phase, the pump was subjected to four 1-gram slugs of contaminant at 36,000 rpm with an outlet pressure of 620 psig. The contaminant mixture for each slug is given in Table IV; the tests were performed in the order noted. The pump was operated for 1/2 hour after injection of the contaminant slug to the pump inlet. The results were encouraging because no measurable flow degradation or increase in input power occurred during or after the injection of the contaminant.

The pump was visually inspected after each cycle to determine the effects of the various types of contaminant. The Arizona road dust and the large silica sand particles produced the only evidence of damage. After Cycle No. 1, a light erosion of the end plates was noted in the area where there is leakage past the ends of the vane tips on the pumping lap space. Damage to the outside diameter of the aluminum axial inducer was also noted. Cycle No. 2 produced some light scuffing on the cam-ring sealing-lap-space area where the clearance between the cam ring and the rotor (0.005 inch) is less than the silica sand particle size. The vane tips were not affected by this light cam-ring scuffing,and they showed no evidence of degradation of the tip load-support capability. The final two cycles produced no additonal changes in the pump components. An inspection after the above experiments revealed that the tip bearing-pad surface finishes were virtually unchanged. The overall cam-ring bore surface finish changed from 0.6 microinch CLA to 0.9-microinch CLA due to a few light scratches which were noted. In the sealing-lap-space area, where the large silica sand particles were crushed between the cam ring and the rotor, the surface finish was a maximum of 2.5 microinches CLA. Light contaminant polishing was noted on the sides of the vane slots in the rotor, but it was not enough to remove the original machining-tool marks.

During the final phase the pump was operated over a speed-pressure schedule while the contaminant was continuously introduced to the

TABLE IV. "SINGLE-PASS" CONTAMINANT SCHEDULE

Cycle No.	Arizona Road Dust (A.C.Spark Plug Co. Part No. 1543637) (gm)	Silica Sand 177-250 microns (gm)	Silica Sand 250-420 microns (gm)	Iron Oxide (gm)	Total Contaminant (gm)
1	1	0	0	0	1
2	0.8	0.1	0.1	0	1
3	0	0	0	1	1
4	0.2	0.025	0.025	0.75	1

inlet at a rate of 12 grams/hour. The speed-pressure schedule was identical to that used during the endurance evaluation except that each cycle was 3 hours in duration. The percentage of time at each condition is shown in Table V. The JP-4 fuel was contaminated essentially as prescribed by MIL-E-5007-C except that the cotton linters, napthenic acid, and salt water were omitted. The latter components were omitted because the basic objective of the evaluation was to determine the abrasive-wear resistance of the fuel-pump hardware. The contamination rate of 12 grams/hour produces an average contaminant density of 40 grams/1000 gallons of fuel pumped. The mixture consisted of 75 percent 0- to 10-micron iron oxide, 5 percent 177- to 420-micron silica sand, and 20 percent coarse Arizona road dust (A. C. Spark Plug Company Part No. 1543637).

The experimental fuel pump was operated for a total of 34 hours at the above conditions. At no time during this period was there evidence of a pump mechanical failure or an increase in the required input power at each condition. There was considerable flow degradation, however, and this is shown in Figure 8 for the 40,000 rpm, 650-psig conditions. The pump was disassembled once during the 34-hour period for a complete inspection at the 16-hour point. This was done to determine why there was a more rapid deterioration in the flow performance after the first 10 hours.

The inspection revealed considerable erosion of the end plates in the area where there is leakage past the ends of the vane tips on the pumping lap space. The start of this erosion had been noted after Cycle No. 1 in the slug tests. The erosion is noted in the photograph presented in Figure 9. The maximum depth of the cavities noted is approximately 0.004 inch. Although additional damage was found on some of the other components, it was not considered serious and should not have affected pump performance. The pivoting vane tips and cam ring bore showed no evidence to indicate relative contact. The performance of the pivoting tips was not affected by the contaminant at this point. Inspection of the tip bearing pads revealed a slight deterioration of the surface finish, but no changes in the pad profile. A light erosion of the leading edge of the tip axially aligned with the two inlet ports was observed. The sealing lap space area also showed additional scuffing from the large silica sand particles and a resultant material removal of 50 microinches at the outer ends of the cam-ring bore. The overall cam-ring bore surface finish had increased to 4.0 microinches CLA.

The end-plate damage appeared to be due to the impingement of the contaminant perpendicular to the end plates. This action probably attacks the Ferro-Tic C binder material (tool steel) and suggests that a low-binder carbide should be used in place of the Ferro-Tic C, which is 50 percent binder. To confirm this, the end plates were refaced with a 0.040-inch-thick layer of tungsten carbide (G. E. Grade 883). The tungsten carbide was bonded to the end plates with a high-temperature-cure epoxy adhesive.

TABLE V. CONTAMINATED-FUEL SCHEDULE

Speed (rpm)	Outlet Pressure (psig)	Time at Conditions (hr)	Percentage of Total Time
26,000	510	1.7	5
30,000	550	3.4	10
32,000	570	8.5	25
36,000	620	15.3	45.
40,000	650	5.1	15
	Totals	34.0	100

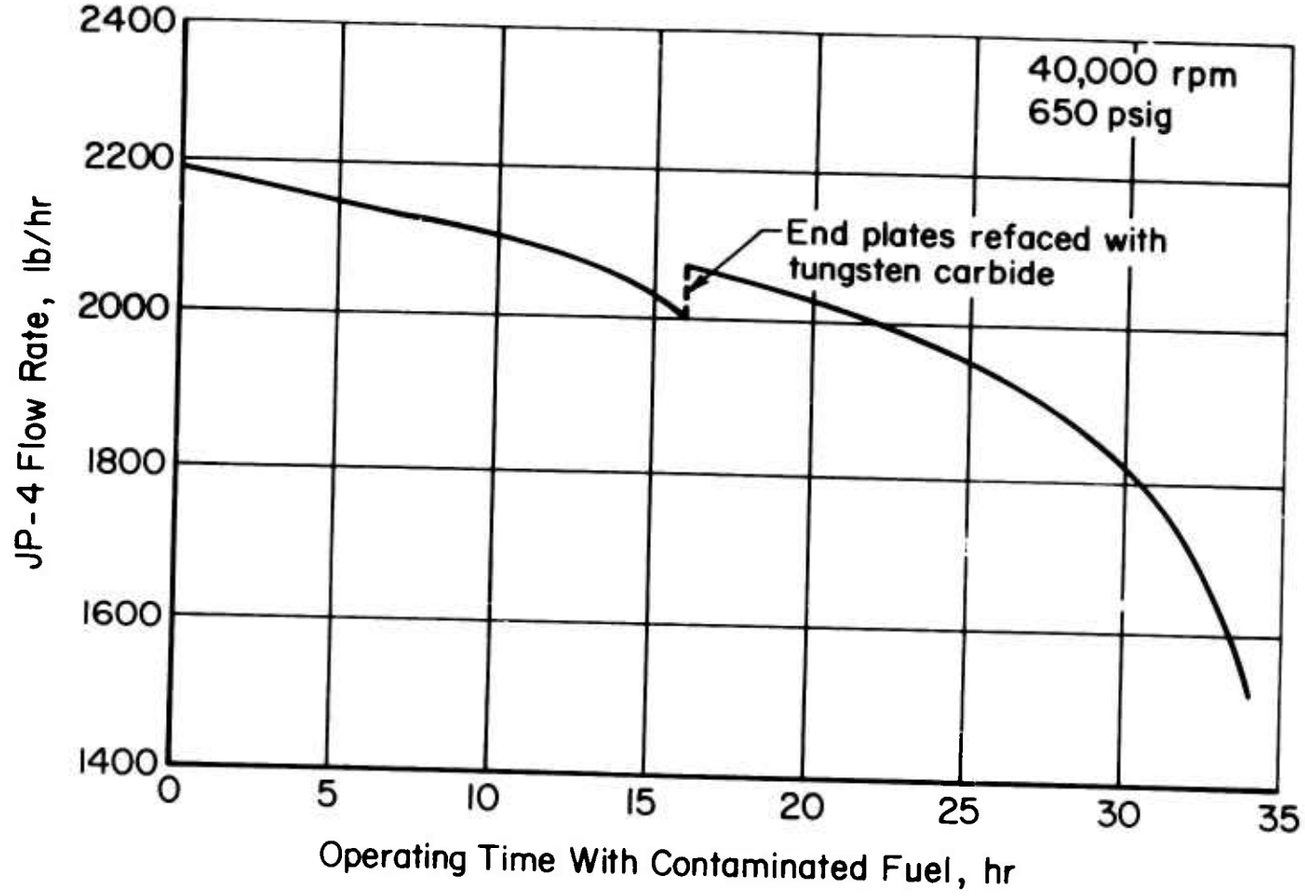

Figure 8. Flow-Performance Degradation During Contaminated-Fuel Evaluation.

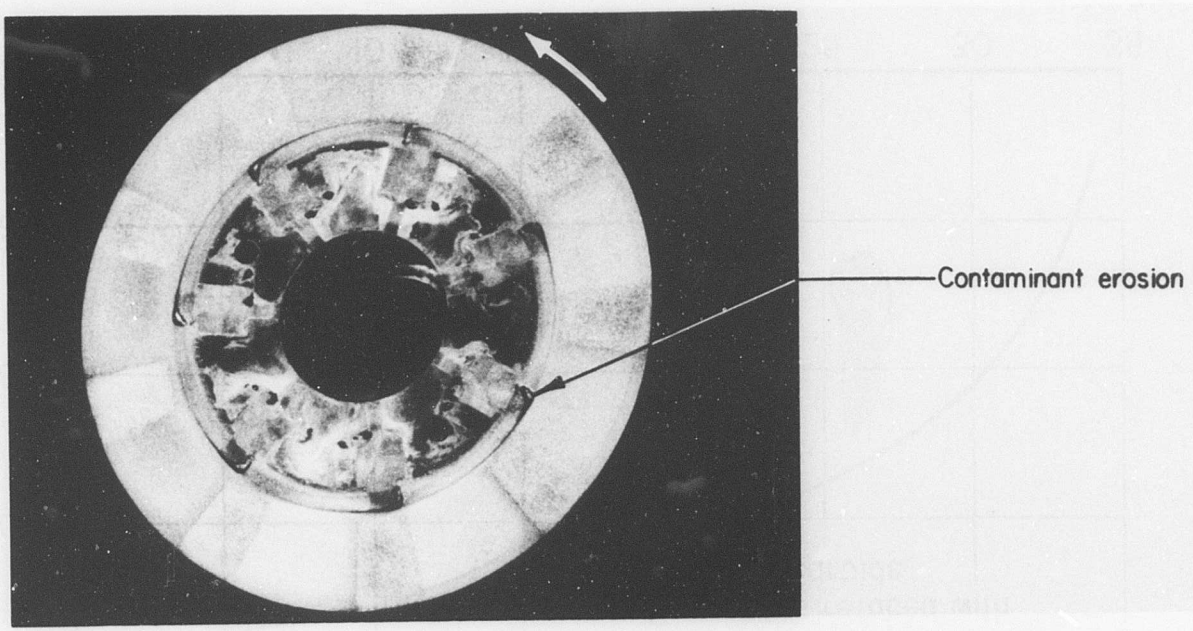

Figure 9. End-Plate Erosion After 16 Hours of Operation With Fuel Contaminated per MIL-E-5007C.

It was intended to reassemble the pump with the same components, except for the refacing of the end plates. It was found, however, that the technique used to bond the tungsten carbide permitted slight distortions in the flatness of the faces when the journals were axially loaded during assembly. This reduced the end clearance slightly, and one vane tip would not stroke properly because of insufficient end clearance. The rotor originally used at the start of the endurance evaluation was then installed because it was slightly longer and permitted proper vane stroking in spite of the end-plate distortion. The performance of the pump was then established after the noted changes using clean JP-4, and the contamination evaluation was continued. The flow performance after the changes is noted in Figure 8. Repairing the end plates did not eliminate all of the first 16-hour flow degradation. It is felt that the remaining flow loss was due to increased leakage past the ends of the tips. The end corners of the tip pads and the edges of the cam-ring bore in the lap-space areas were chamfered by the contaminant. This still permitted excessive leakage past the ends of the tips because a small orifice that leaked continuously was produced. The increase in the flow rate after the refacing of the end plates represents the contribution of the original end plate damage to the total flow degradation experienced during the first 16 hours.

The flow performance continued to degrade with continued operation. During the last 3 hours of operation, the rate of degradation increased considerably, and this led to the decision to terminate further evaluation. After 34 hours, the volumetric efficiency had decreased from the original 88 percent at 40,000 rpm, 650 psig, to 60 percent. This represents a total leakage of 1020 lb/hr, or 40 percent of the theoretical capacity of 2540 lb/hr at 40,000 rpm.

The power required to drive the pump actually decreased during the contamination evaluation. This is due to the fact that the flow required by the vane stage from the centrifugal stage decreases as the vane-stage internal leakage increases. This represents throttling of the centrifugal stage, which requires less power at lower flow conditions. The decrease in the required centrifugal-stage power represented 100 percent of the decrease in total pump inlet power. The required vane stage power remained essentially constant over the 34-hour period.

A complete inspection of the components was made after termination of operation. Considerable damage was noted on all components, except for the refaced end plates. There was evidence that the tip performance was marginal, and areas of relative contact between the tips and the cam-ring bore were noted in the lap space, particularly at the axial center of the cam ring. The complete hydrodynamic film had not been destroyed, however, because this would have produced a considerable increase in the power required to drive the vane stage. The above condition was quite encouraging, however, considering the level of damage encountered by the components.

The cam-ring bore straightness, which was originally within 5 microinches, was found to have low areas with a maximum depth of 100 microinches.

Material removal at the ends of the sealing-lap-space area was as much as 100 microinches. The overall cam-ring bore surface finish had increased to a range of 6.5 to 12.0 microinches CLA. All vane tips had as much as 80 microinches removed from the bearing-pad surface, and the wear was axially distributed to reflect the location of the inlet ports. Where the two ports are located, very little material removal was noted. This condition is shown schematically in Figure 10. The bearing-pad profile was also changed in the highly worn areas. The pad radius in these areas was found to be approximately the same as that of the cam ring, and in some cases it was larger.

The wear pattern on the vane tips reduced the effective bearing length of the tip to approximately 25 percent of the tip length on the lap spaces. In the port areas, only the damaged portions of the tip length were available for load support because of the location of the ports relative to the erosion. It appears that the tips were able to operate under such conditions only because of the extremely stiff bearing design, which permits overloading of the bearing without large reductions in the minimum film thickness.

The axial alignment of the erosion of material on both the tips and the lap spaces would also produce a leakage path across the tip surface in this area. This condition, once formed, probably permits acceleration of the erosion because more contaminant is allowed to enter the hydrodynamic film. It is felt that the potential for accelerated wear justified the marked increase in erosion noted during the last 18 hours as compared with the relatively light erosion noted during the first 16 hours.

The wear on the vane assemblies was considerably more than that encountered during all previous operation on clean fuel. The wear represented an average weight loss of 2.6 milligrams for the outer vanes, 1.6 milligrams for the tips, and 1.5 milligrams for the inner vanes over the 34-hour period. The major damage occurred on the leading edges of all these components. For example, in the vane socket area, no measurable damage occurred on the trailing portion of the socket where the tip is usually in intimate contact and the clearance is removed. On the leading portion, the clearance formed permitted the contaminant to enter and cause wear as the tip rotated. The same is true for the sides of the outer vane. Local wear on the leading edge produced as much as 500 microinches of material removal. The overall outer-vane width was reduced approximately 100 microinches. The wear pattern developed on the trailing edge during endurance testing showed negligible change, however. In addition, chipping of the leading edge ends of the outer vanes in the socket area was noted on two vanes. This was probably due to the fact that much of the contaminant appeared to flow to the ends of the rotor, and this area on the vane must push the larger silica sand particles through the sealing lap space/rotor clearance (0.005 inch).

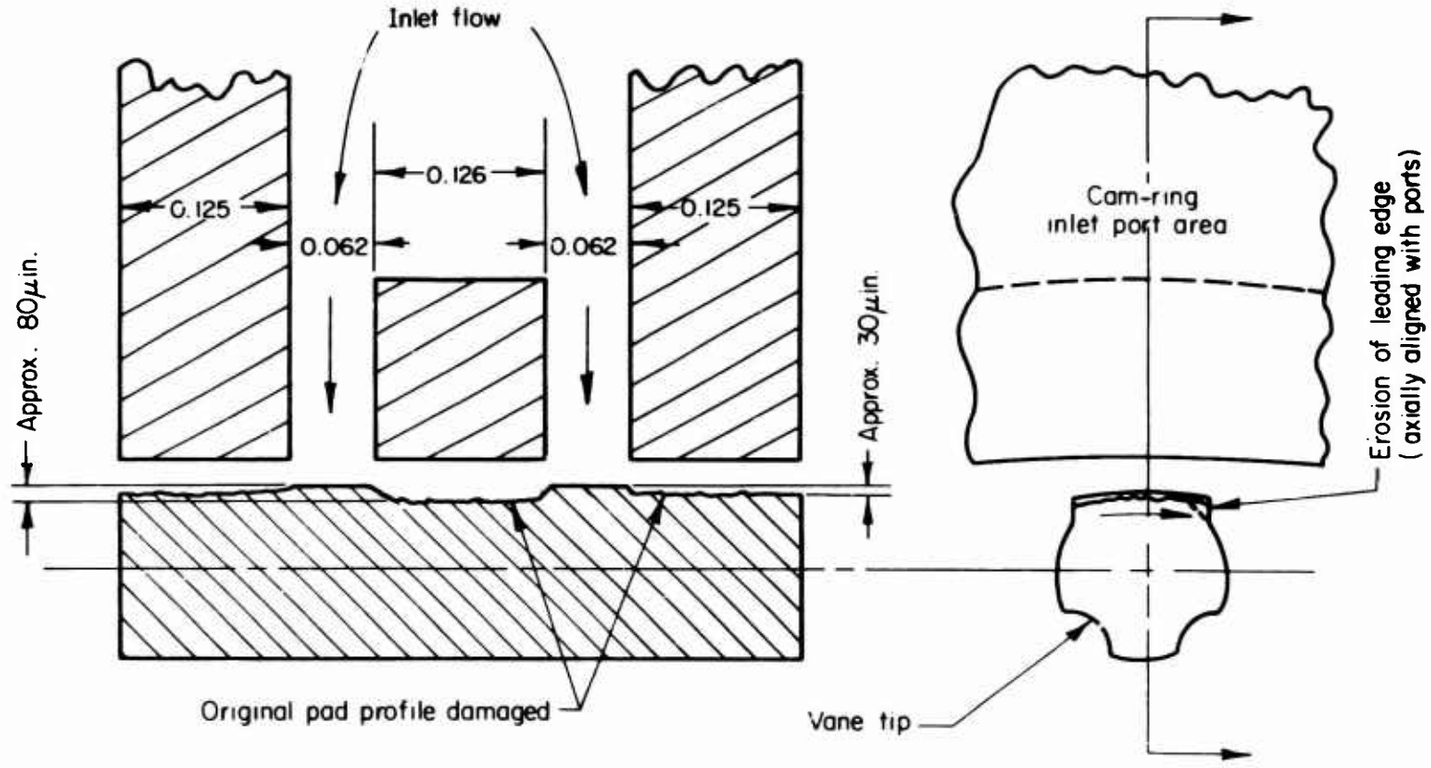

Figure 10. Schematic of Vane-Tip Wear During Contaminated-Fuel Evaluation.

The rotor proved to be the most susceptible to damage from the contaminated fuel. The outer vane slot widths increased as much as 0.002 inch on both rotors. This should not have affected pump performance, however. The inner-vane slot widths had negligible wear on the first rotor, but three consecutive inner-vane slots on the second rotor had localized increases in width from 0.001 inch to 0.005 inch. The remaining four slots were approximately the same as the first rotor. The inner vanes did not have comparable wear, and their overall width and the trailing-edge wear pattern noted during endurance testing remained essentially unchanged. It is felt that the increased leakage produced on the inlet portion of the pumping cycle by the much larger inner vane clearance contributed a significant amount of the total flow loss encountered. Unfortunately, no explanation of why just three consecutive inner-vane slots wore has been established.

The chamfering of the edges of the cam-ring bore continued during the final 18 hours, and a maximum 0.010-inch chamfer was formed in the pumping lap-space area. The end-plate erosion noted with Ferro-Tic C was virtually eliminated by the use of tungsten carbide. Only very small cavities with a maximum depth of 170 microinches were formed. The thrust-bearing performance was excellent and no damage was encountered. The journal-diameter wear was also low, with a maximum diametral reduction of 100 microinches. The bronze sleeves started to show some deterioration after 34 hours, but the overall journal bearing performance was good. The sleeve diameters were tapered with a maximum diametral increase of 700 microinches where high-pressure fuel enters the clearance. At the low-pressure ends, the wear was negligible. This change in diameter allowed increased bearing leakage, but it represents only a small percentage of the total flow loss.

It should be again noted that although the flow performance was unacceptable with contaminated fuel, the mechanical performance remained good in spite of considerable deviation from the ideal in the component geometrical configurations.

Discussion of Performance Results

The experimental fuel pump has proven capable of meeting both the overall program objectives and the actual performance goals outlined at the start of the program; an exception is its ability to withstand long-term exposure to contaminated fuel. The results demonstrate that the pump has turbine-speed capability with low-viscosity fluids without sacrificing the endurance performance of the equipment.

The required fuel flow rates at design pressure have been achieved for both light-off and 100-percent speed (40,000 rpm) conditions. In fact, the 100-percent speed fuel flow requirement of 2000 lb/hr was exceeded at the 900-psig overpressure condition. The flow-performance curves (Figure 6) show that the pump leakage rate is essentially constant

and independent of changes in pump speed. The maximum fuel temperature rise of 10°F at the 100-percent speed conditions represents a 50-percent reduction from that obtained during the previous research program. Approximately 70 percent of the temperature rise is generated by the centrifugal stage, which has a 29- to 33-percent overall efficiency over the pump speed range. The centrifugal-stage efficiency is three times greater than previously obtained due to improvements in the diffuser design.

The maximum test speed of 49,500 rpm established that the pivoting vane tip is capable of operating at surface speeds as high as 180 fps with significant load-carrying ability (122 lb/in.). The contaminated-fuel experiments also demonstrated that this tip is not catastrophically sensitive to contamination damage. It verifies that the pivoting tip can perform its function of reducing vane drag at much less than the theoretically ideal conditions. Although the pump was operated for only 2 hours at speeds above 40,000 rpm, the results were positive at these speeds and it appears that the upper speed limit of the tip concept has not been reached.

The distribution of the pump input power at various operating conditions is outlined in Table VI. It is important to note the low power loss assigned to the drag of the hydrodynamically lubricated pivoting vane tips. On the basis of the early pump performance results obtained when hydrodynamic film breakdown occurred at the 25,000-rpm, 500-psig conditions, it is estimated that this power loss would be as much as 25 times greater using boundary-lubrication techniques. The estimated coefficient of friction, based on the measured power loss, for boundary lubrication is 0.055. The coefficient of friction for the hydrodynamic tip is 0.002 when estimated from power data taken at 49,000 rpm.

During the 25,000-rpm tip failures, the input power required to drive the pump increased from 2.2 hp to 3 hp. The additional loss of 0.8 hp severely penalizes overall pump efficiency and demonstrates the need to maintain the hydrodynamic film. Even though the carbide material used for the tips and cam ring is quite durable, the above failure also caused enough scoring of the respective surfaces to indicate limited endurance capabilities at the 90-fps surface speed.

The overall pump efficiency is not high, as noted in Table II. Considering, however, the relatively low pump-flow capacity and the extremely high rotational speeds, it is still respectable. The centrifugal charging pressure appears to be conservative, and once the minimum requirements of the vane stage are experimentally determined, it may be possible to require the more efficient vane stage to supply a greater percentage of the higher speed pump head. This, plus optimization of the bearings and the leakage parameters, should allow for some improvement in the overall efficiency. The performance results indicate that smaller bearings are possible, since it appears that the present bearings are conservative in design for the loads they are required to support. The smaller

TABLE VI. POWER DISTRIBUTION

Item	Power Consumption (hp); Percentage of Total Input Power				
	15,000 rpm, 330 psig	30,000 rpm, 545 psig	40,000 rpm, 650 psig	40,000 rpm, 900 psig	45,000 rpm, 650 psig
Power to drive thrust and journal bearings	0.12; 16	0.46; 15	0.82; 14	0.82; 12	1.04; 14
Power to drive centrifugal stage	0.15; 20	1.16; 37	2.74; 47	2.65; 39	3.92; 53
Flow losses in vane stage	0.03; 4	0.27; 9	0.64; 11	0.64; 9	0.91; 12
Vane tip drag (7 vanes)	0.02; 2	0.07; 2	0.12; 2	0.12; 2	0.15; 2
Theoretical hydraulic power developed by the vane stage	0.44; 58	1.17; 37	1.55; 26	2.53; 38	1.44; 19
Total input power (sum of above individual items)	0.76;100	3.13;100	5.87;100	6.76;100	7.46;100
Total input power (measured during evaluation)	0.73	3.1	5.9	6.8	7.5
Total hydraulic output power from pump	0.39	1.38	2.25	2.85	2.54
Hydraulic output of vane stage	0.35	1.0	1.36	2.03	1.29
Hydraulic output of centrifugal stage	0.04	0.38	0.89	0.82	1.25
Overall efficiency, %	53	43	38	42	34
Volumetric efficiency, %	90	86	88	80	89

bearings would result in lower mechanical-power losses. It is doubtful that the flow losses in the vane pump can be reduced significantly because of the very high fluid velocities at the high rotational speeds.

Generally, reduced efficiency is the major trade-off required to achieve high rotational speeds. This takes the form of increased mechanical and flow losses. The use of the pivoting vane tip plays a major role, however, in keeping the losses acceptable as well as providing the necessary endurance qualities.

The vane redesign proved successful during the performance testing. The previous operational deficiencies, such as undervane impact conditions and high outlet pressure pulsations experienced with the earlier design, were successfully eliminated. The only limitation noted with the present design is its low vane engagement ratio, and this did not affect the pump's general performance.

The contaminated-fuel experiments generally indicate that to endure the MIL-E-5007C contaminated-fuel requirements, the component materials must be more erosion resistant than Ferro-Tic C. It should be pointed out, however, that the 12 grams/hour of contaminant rate was maintained in spite of a decrease in the total number of gallons pumped. At the start of the test, this represented a contaminant density of 40 grams/1000 gallons of fuel pumped. After 34 hours, this had increased to 60 grams/100 gallons of fuel pumped, which exceeds the specification requirements. It is felt that the increasing contaminant density is one reason for the acceleration of the component damage with time. Although the flow performance in the contaminated environment is not acceptable, the results indicate that the basic design concepts incorporated in the experimental fuel pump are not unduly sensitive to this environment. On the basis of the superior performance of the tungsten carbide end plates, it would appear that its use in all other vane-stage components would practically eliminate the flow performance difficulties. A tungsten carbide rotor appears impractical, however, and compromises will be required. The experience gained with the performance of the pivoting tip makes the use of tungsten carbide vane-assembly components reasonable, in spite of its high density.

CONCLUSIONS

The experimental performance results obtained during this research program have been positive. The operational deficiencies experienced with earlier hardware which used the same basic technologies have been eliminated. The present experimental fuel pump represents a significant step toward the development of flight hardware capable of operating at engine shaft speed. It meets the basic performance requirements of a main-engine fuel pump typically required on small, high-speed gas-turbine engines.

It presently appears that a variable-displacement capability could be developed directly from the present hardware without altering the

established high-speed capabilities. This is important because significant gains in overall fuel-system performance can result from the use of a variable-displacement fuel pump. In addition, the basic configuration appears to provide for performance over a relatively wide range of pump capacities and speeds. It is felt that the configuration is best applied to low-capacity, very high-speed fuel pumps, but larger-capacity, lower-speed single-lobe vane pumps are feasible. It would appear, however, that the basic concepts should be applied only to pumps with 100-percent design speeds greater than approximately 15,000 rpm to obtain the necessary journal-bearing load capacity with low-viscosity fluids.

The heart of the pump, the pivoting vane tip, provides definite endurance and power-consumption advantages. Both the experimental results and theoretical analyses indicate that even higher surface speeds can be achieved in spite of the poor lubricating qualities of the turbine fuels. The maximum speeds achieved will likely be limited by the level of flow losses in the vane stage which produce unacceptable efficiency characteristics. This efficiency limit would be reached at much lower speeds, however, if it were not for the low levels of vane-tip drag made possible by the use of the pivoting vane tip.

The pump is capable of operating at engine shaft speeds in the contaminated-fuel environment. To maintain the flow-performance characteristics during long-term exposure to this environment, it appears necessary to incorporate the use of tungsten carbide for the vane-stage components. The use of tungsten carbide cermets will generally increase the manufacturing cost of the pump components, and should be considered only when absolutely necessary, since they are not required to achieve high-speed endurance characteristics in the fuel pump. The pump can accept high-density slugs of contaminant without performance degradation even though less contamination resistant materials were incorporated in the design.

RECOMMENDATIONS

Because of the positive results obtained during this research program, it is recommended that the basic concepts generated be considered in the planning of any future programs dealing with high-speed pump development. This applies not only to fuel pumps, but also to high-speed hydraulic pumps where it is necessary to maintain reasonable levels of mechanical efficiency. It is suggested that the initial effort be directed toward the development of hardware with variable-displacement capability, particularly for fuel-system applications which require high turn-down ratios and minimum fuel temperature rise. In addition, it is felt that future hardware should also be evaluated at higher fuel pressures (up to approximately 1500 psig) to insure that the basic concepts can function properly across the full pressure range required by various fuel-system applications.

Although the performance of the basic configuration was highly encouraging during this program, details remain which should be investigated in

greater depth. The following is a list of such details and suggestions on how they should be dealt with in the future:

(1) The optimization of vane-stage component materials to insure satisfactory flow performance in the contaminated-fuel environment. Although tungsten carbide cermets appear to be ideally suited, less contamination-resistant materials may suffice for certain components and allow minimization of production costs. It is suggested that this be considered once a particular pump application has been defined, rather than for a generalized configuration.

(2) The experimental determination of the performance characteristics of the pivoting vane tip to establish its operational limits over a wider range of speeds, loads, and fluid viscosities than experienced during the present program. Information on the required level of tip geometric accuracy should be developed before attempting to apply the tip to an actual flight hardware design. The experimental evaluation of the generalized tip configuration discussed in Appendix II should also be considered, because of the apparent benefits that it may provide.

(3) The optimization of the centrifugal stage design. In conjunction with this effort, the charging pressure needed to provide proper vane stage filling should be experimentally determined. This would probably be best handled, however, in conjunction with each particular fuel system.

(4) The investigation of alternative or improved vane designs, with the basic objective being to provide larger vane engagement ratios in pumps with small rotor diameters.

APPENDIX I

LABORATORY SETUP AND EQUIPMENT

A 10-hp motoring dynamometer with a maximum speed of 6000 rpm was used to drive the experimental fuel pump. To achieve the pump speeds, a flat belt drive speed-increaser system was used which provides a 9.5/1 speed increase. The pump was directly driven through keys by an extension to the high-speed pulley. An aluminum shear-pin failure link was used to disconnect the drive system in the event of a pump failure or overload. The keys were provided to limit the axial loading of the pump thrust bearings by the speed-increaser system. The drive shaft assembly was sized to place all critical shaft speeds above 50,000 rpm.

The speed-increaser system and the experimental fuel pump assembly are shown in Figure 11. The torque required to drive the speed-increaser system is essentially constant across a 25,000- to 50,000-rpm speed range. This torque is approximately 10 percent of the torque required to drive the fuel pump at the 40,000-rpm, 650-psig conditions. The low torque level with respect to the required pump drive torque permits a more accurate determination of the required fuel pump input power. The torque required to drive the speed-increaser system was checked frequently during the test program to insure that no variations occurred. The overall system proved to be quite reliable at speeds up to 40,000 rpm. At higher speeds, considerable belt slippage was encountered because of the increasing power required to drive the pump. It was difficult to maintain belt tension for long periods at the higher speeds because of continual stretching of the belt. These problems required that all endurance testing be conducted at a maximum speed of 40,000 rpm.

The fuel pump was instrumented so that flow rate; inlet, interstage, and outlet pressures; inlet and outlet temperatures; speed and input power could all be monitored continuously during the test program. The photograph of the laboratory control room in Figure 12 shows the arrangement of the instrumentation and the dynamometer controls.

The pump outlet fuel was filtered using a 10-micron nominal filter prior to being returned to the reservoir. The test fluid used for all the experimental pump evaluations was JP-4 turbine fuel with a specific gravity of 0.75 and a kinematic viscosity of 0.9 centistoke at 80°F. The flowmeters were calibrated using the same fuel as that used for the test program. They were calibrated before the test program was initiated and after completion of the contaminated fuel experiments. No changes in the flowmeter calibration curves occurred over this period of time.

The continuous belt system used to introduce contaminant into the pump inlet during the contamination fuel evaluations is shown in Figure 13. The motor-driven belt introduced contaminant at a rate of 12 grams/hour. The contaminant dropped off the belt and down a tube in the reservoir. The tube was located on the axis of a funnel in the reservoir and directed the contaminant to the outlet area of the funnel. The funnel

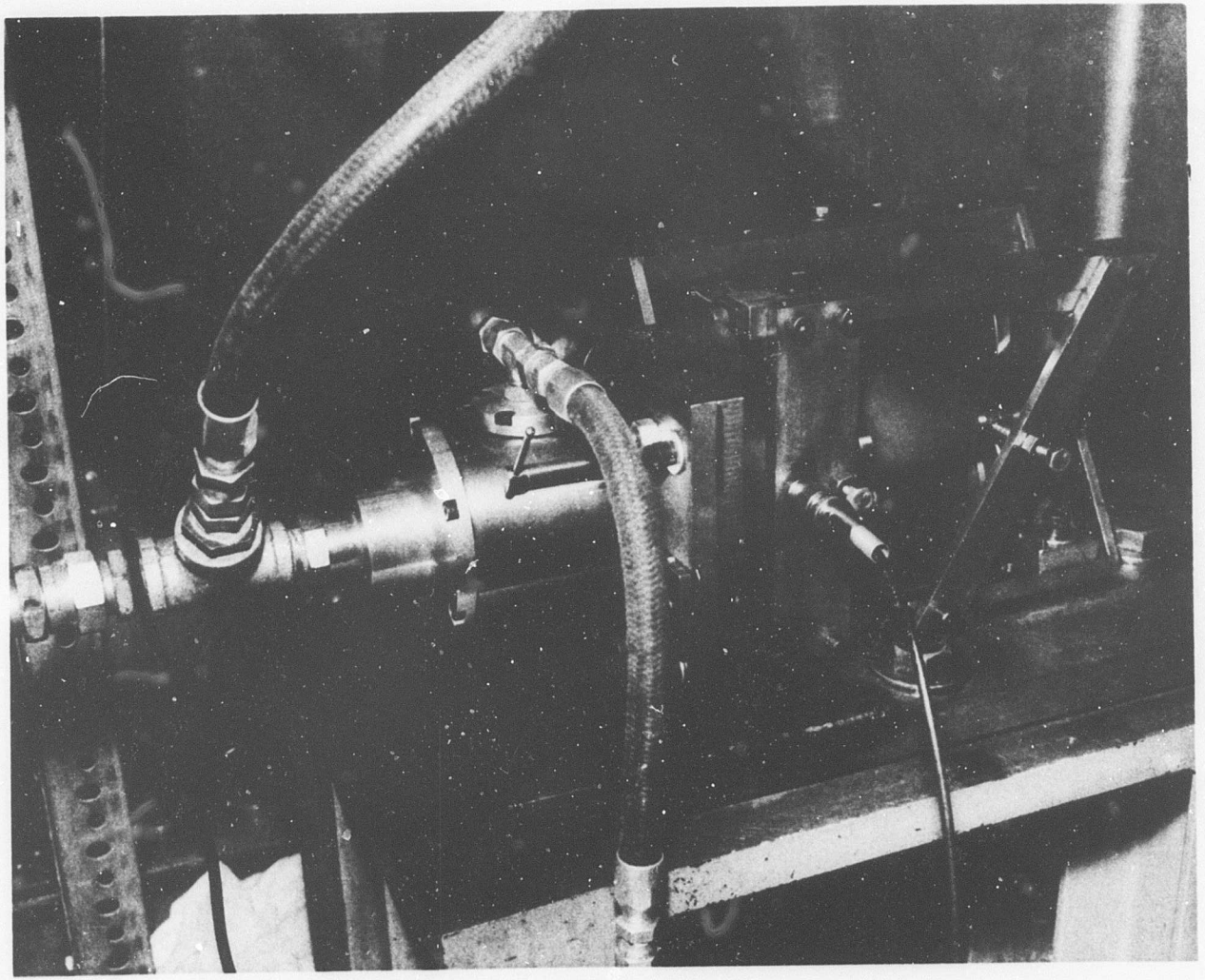

Figure 11. Speed-Increaser System and Experimental Fuel Pump.

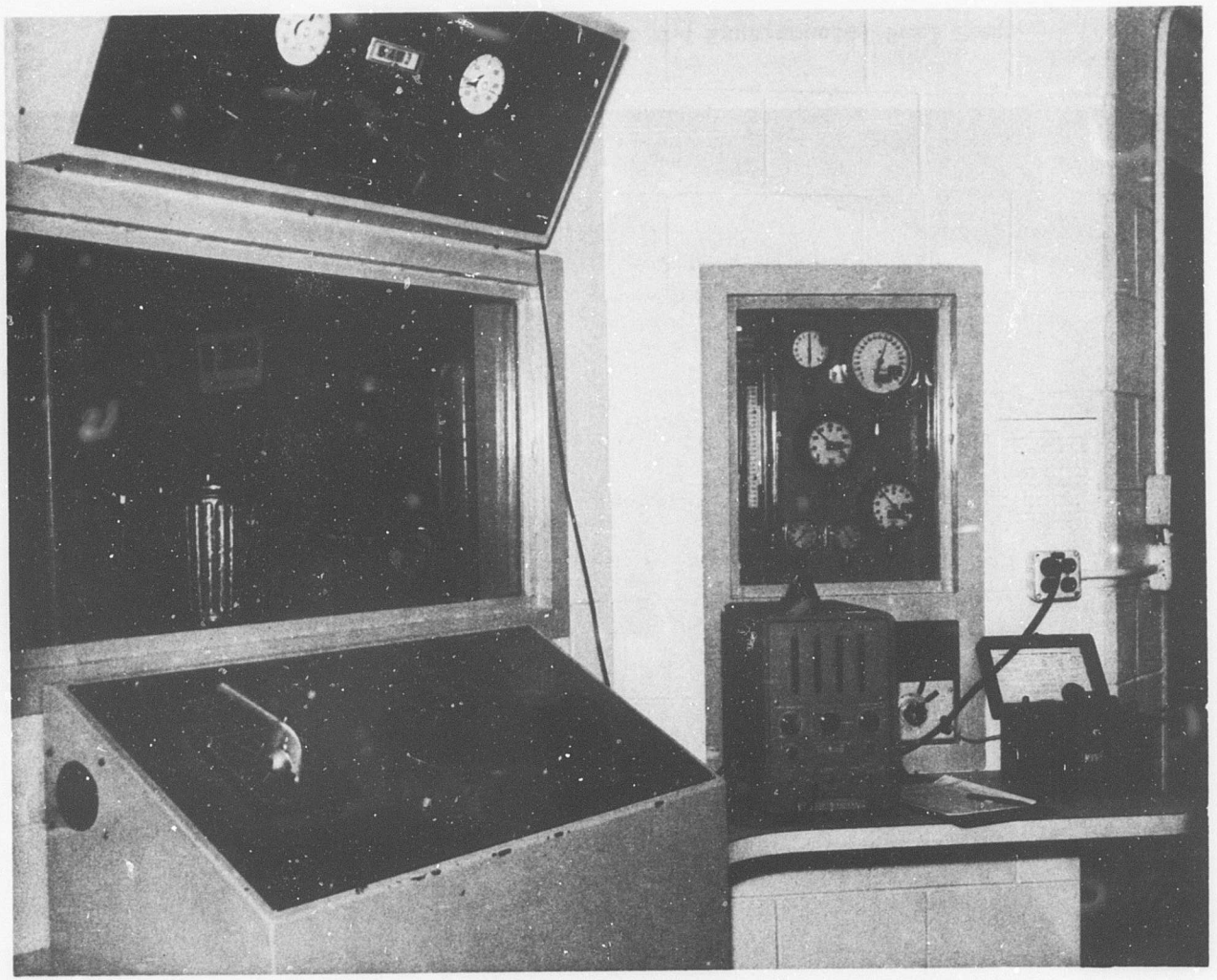

Figure 12. Laboratory Control Room and Pump Instrumentation.

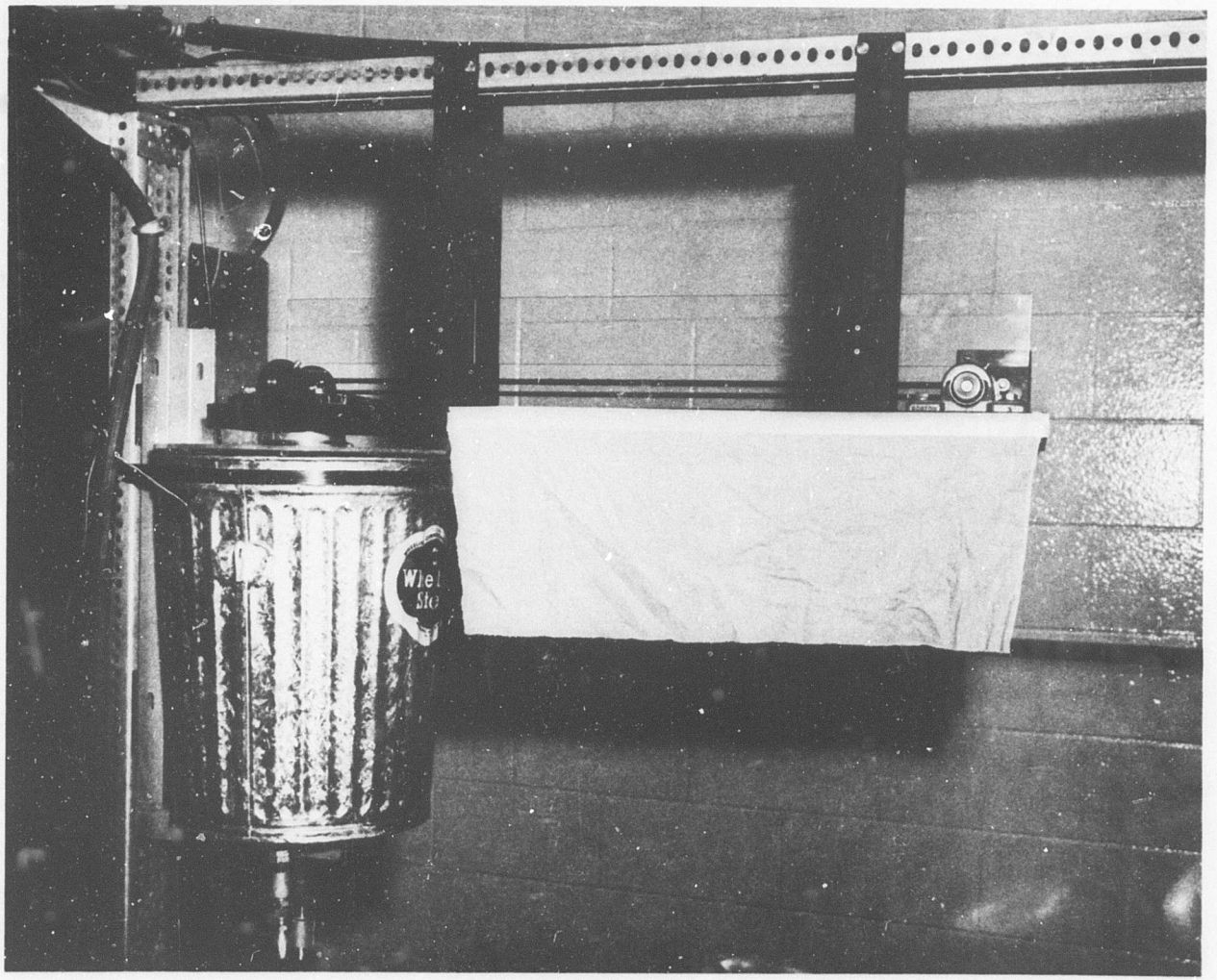

Figure 13. Contaminant Feed System and Fuel Reservoir.

outlet was connected directly to the pump inlet, insuring that all the contaminant was introduced into the pump inlet in a uniform manner. Fuel was returned to the reservoir at its base and the reservoir level was maintained above the top of the funnel.

APPENDIX II

DETAILS OF VANE-TIP DESIGN ANALYSIS

The objective of the pivoting vane tip concept is to provide a vane tip which acts as a hydrodynamic thrust bearing capable of supporting all radial vane loading without contact between the vane-tip surface and the cam-ring surface. The loading is supported by the self-generated hydrodynamic pressure produced in the fluid film between the tip and cam-ring surfaces. The generation of the hydrodynamic film allows for operation at increased relative surface speeds between the tip and cam ring with the corresponding reduction in friction and component wear rates normally characteristic of hydrodynamic lubrication.

The pivot design provides the necessary tip rotational freedom that allows the tip bearing surface to follow the cam-ring surface as the angle between the normal to the cam surface and the vane center line varies during one complete rotational cycle of a vane. This rotational freedom also provides the tip bearing with the self-adjusting taper angle capability of a tilting-pad bearing to produce optimum operation over a wider range of operation conditions.

The pivoting vane-tip design for the fuel pump is centrally pivoted. For centrally pivoted pad bearings, there must be a relative crown between the bearing pad and the thrust surface it runs against in order to produce a hydrodynamic film. In the usual applications,the thrust surface is flat and the bearing pad is slightly convex. The convex crown on the pad is approximately the same magnitude as the minimum film thickness for maximum load support. In the pump application, the thrust surface is the circular cam ring surface. To produce the relative crown between the bearing pad and the cam ring, the pad has a slightly smaller radius than the cam ring. The bearing pad need only be convex relative to the cam ring, but a true radius is much easier to produce in practice.

A computer program developed at Battelle's Columbus Laboratories was used to analyze the application of the bearing to a vane pump. The program is based upon the solution of the Reynolds equation for the no-side-flow condition. This two-dimensional analysis neglects bearing side flow along the length, but the relatively long vane-tip length in comparison to the pad width makes this assumption reasonable. The additional assumptions involved are that the fluid viscosity is considered constant and that the fluid is incompressible. These assumptions are realized when low-viscosity fluids such as water are used. Previous Battelle research with JP-4 turbine fuel has also indicated good correlation with this theoretical approach.

The resulting load capacity per unit length developed using this analysis is given by

$$W = C \frac{\mu U B^2}{h_o^2} \qquad (1)$$

The load variable (C) is a function of the relative surface profiles as defined by the parameters δ and the minimum film thickness (h_o). δ is defined as follows:

$$\delta = \frac{B^2}{8} \left[\frac{1}{R_t} - \frac{1}{R_{cr}} \right] \qquad (2)$$

The relationship between the load variable (C) and the ratio δ/h_o is given in Figure 14. This curve was developed from the computer analysis of two completely different tip geometries to demonstrate that the load variable is only a function of δ/h_o and independent of tip surface speed (U), and the geometrical size. It is a theoretical plot and therefore does not include the effects of temperature rise in the film of fluid and the resulting decrease in fluid viscosity. This nondimensional curve can be used to determine the tip design for any vane pump as long as it is centrally pivoted and the height of the pad surface from the pivot point is relatively small (less than approximately 0.050 inch). The analysis defines the parameters which allow the vane tip to be evaluated independently of the resulting pump diameter.

The maximum load support is obtained when the ratio of δ/h_o is approximately 0.5. Once a tip radius is chosen, then the maximum load variable (C) is obtained at only one minimum film thickness (h_o). For the fuel pump, the tip radius was chosen so that the load capacity is essentially optimized when the operating minimum film thickness is in the 20- to 35-microinch range. This range of minimum film thicknesses is required in order to support the anticipated radial vane loads with a bearing size consistent with the overall pump geometry. Previous experience had indicated that a pivoting tip of reasonable geometric accuracy could be expected to operate at theoretical minimum film thicknesses as small as 20 microinches.

The 0.387-inch tip radius and the 0.395-inch cam-ring radius produces a δ = 24 microinches for the fuel-pump tip-bearing design. The resulting theoretical load capacity for a tip surface speed of 180 fps is shown in Figure 15. This bearing design is extremely stiff within the anticipated operating film-thickness range; and a bearing is provided that operates at a nearly constant film thickness over a wide range of loads. This bearing performance is obtained at all angular positions of a vane during the pumping cycle, and it is possible to achieve this condition only because the cam-ring radius of curvature is constant. The minimum theoretical film thickness anticipated for the fuel-pump design was 26 microinches, and it occurs on the inlet port at 49,500 rpm. The bearing load support at this point is 122 lb/in. of bearing length.

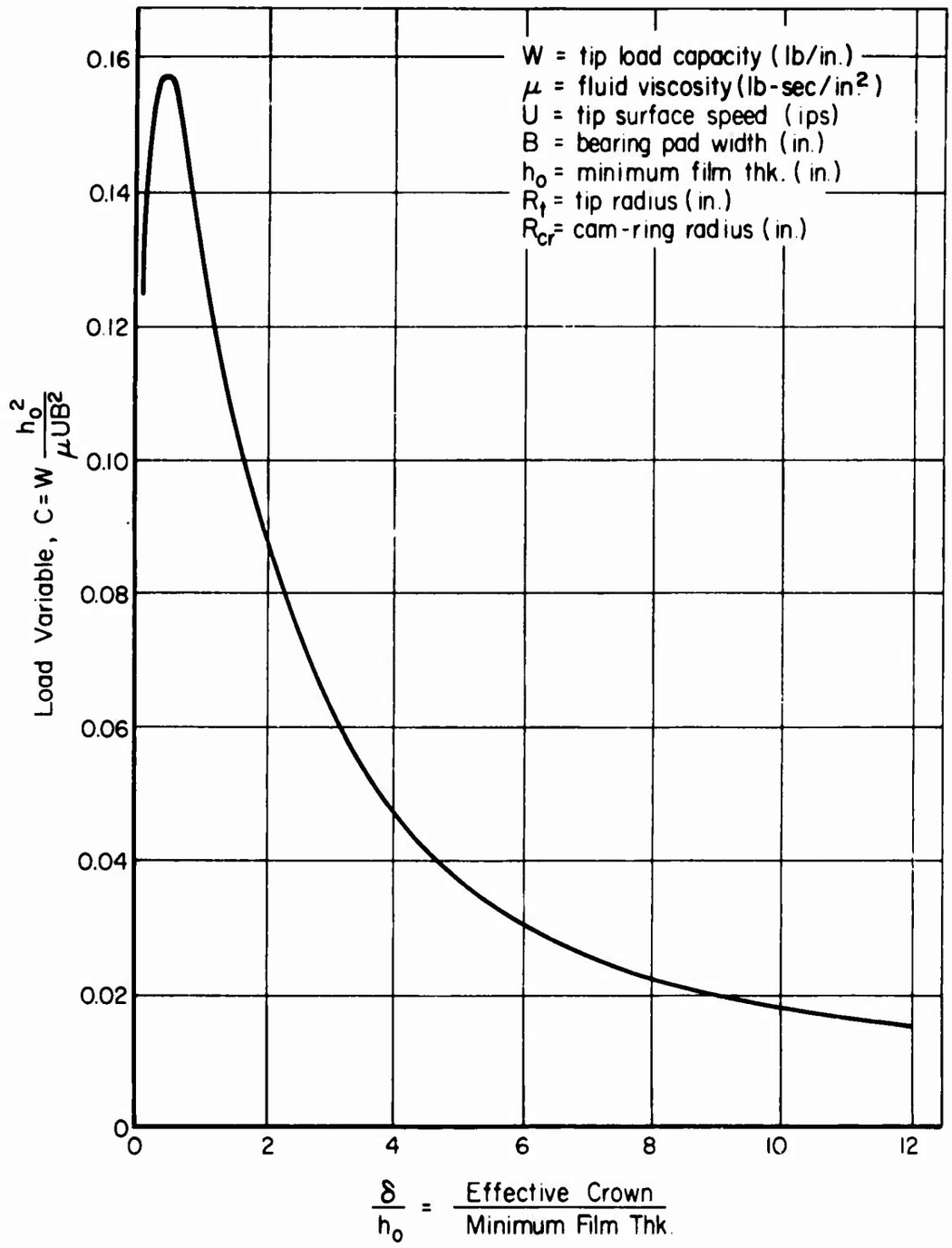

Figure 14. Load Variable Versus Effective Crown to Minimum-Film-Thickness Ratio for a Centrally Pivoted Pad Bearing.

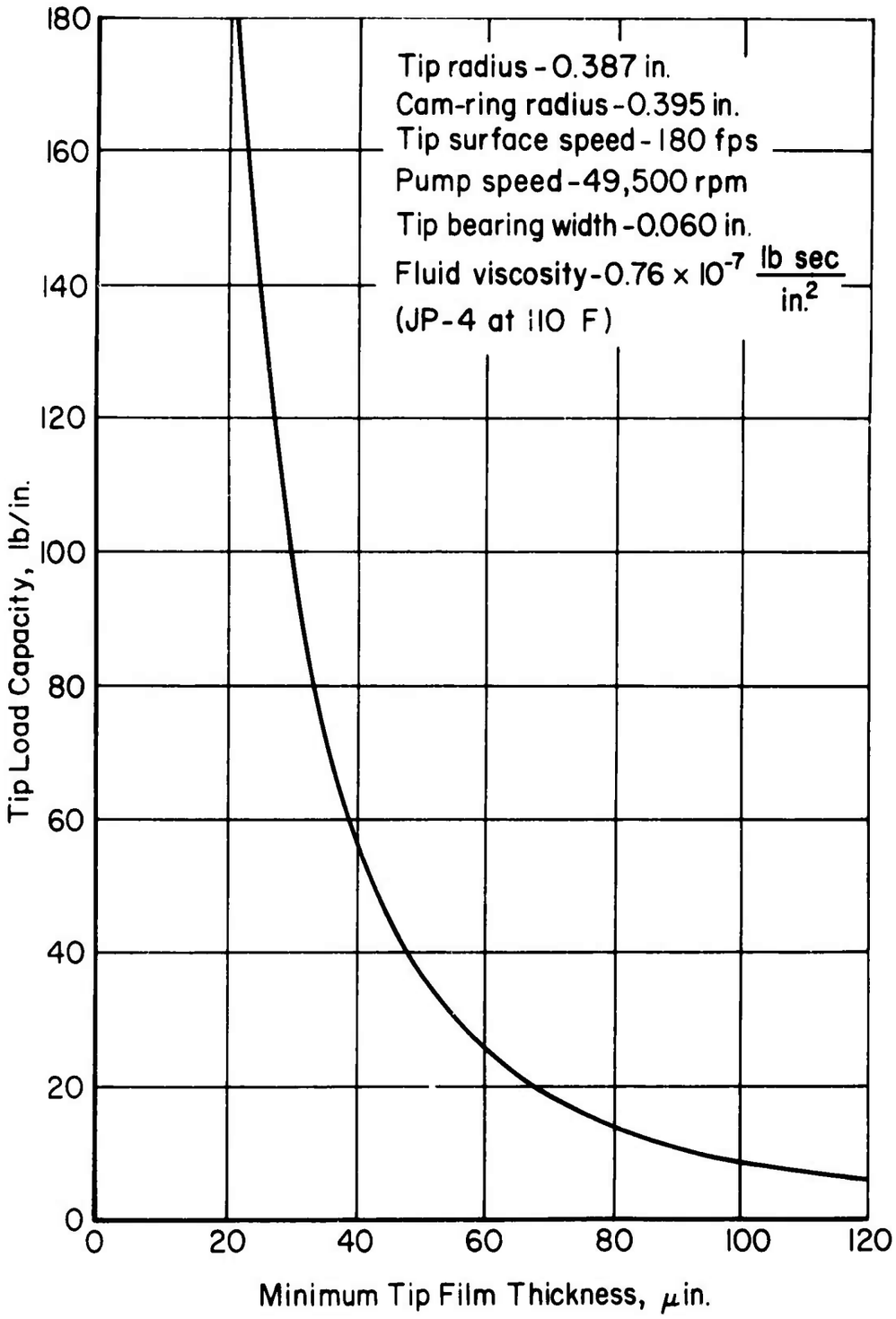

Figure 15. Tip Theoretical Load Capacity at 180 FPS.

Since the vane tips in a vane pump are subjected to differential pressure across their width, the design must incorporate the necessary features which insure that the net hydrostatic rotational moment applied to the tip is essentially zero for all operating conditions. A pivoted-pad bearing exposed to a uniform hydrostatic pressure field will automatically rotate to a position of stable equilibrium. Equilibrium occurs when the resultant force produced by the hydrodynamic pressure profile passes through the pad pivot. This position also provides the proper orientation between the tip bearing surface and the cam-ring surface to promote the hydrodynamic load-carrying pressures in the film. To maintain this orientation, the hydrostatic moments created by the pressure differential must be counterbalanced by additional moments proportional to the magnitude of the pressure differential. In addition, it is necessary to insure that if the tip is disturbed from the equilibrium position, then the resulting moment created be of proper direction so as to return the tip to the equilibrium condition.

The generalized pivoting vane-tip configuration shown in Figure 16 insures that the above conditions are met. Hydrostatic pressure acting against Surfaces 1, 2, and 3 produce moments which counterbalance the hydrostatic moment generated by the hydrostatic pressures acting on the bearing surface when the vane tip is subjected to a pressure differential. These moments automatically reverse direction in phase with the bearing pad surface moments. The higher the magnitude of the hydrostatic pressure relative to the self-generated hydrodynamic pressure, the more critical the need to maintain an essentially zero net hydrostatic moment. This condition occurs in the fuel pump at the low-speed light-off conditions. At higher speeds, the hydrodynamic pressure is dominant and capable of producing stable equilibrium in spite of a net hydrostatic moment.

The tip configuration used in the fuel pump is a specific example of the generalized tip shown in Figure 16. The fuel-pump tip only requires Surface 1 to provide the counterbalance moment and has a pad width smaller than the pivot socket diameter. Continuing efforts directed toward improving the present tip design, however, resulted in a generalized configuration which appears to be superior. It was found that a tip with a bearing pad width greater than the socket diameter could be designed to be rotationally stable for the fuel pump application. Surfaces 1 and 2 actually provide a hydrostatic moment greater than the hydrostatic moment applied to the bearing surface. The addition of Surface 3, however, produces a moment which makes the net hydrostatic moment essentially zero.

The resulting tip design therefore has significantly increased load support (larger bearing pad width) without producing additional acceleration loads. This is due to the fact that the pad width can be made as large as the present vane width without appreciably increasing the vane-assembly mass. For a 0.110-inch pad width, the rotational stiffness of the tip bearing is increased to 4.6 times that of the present tip. As a result, the maximum stable operating film thickness is increased from 70 microinches

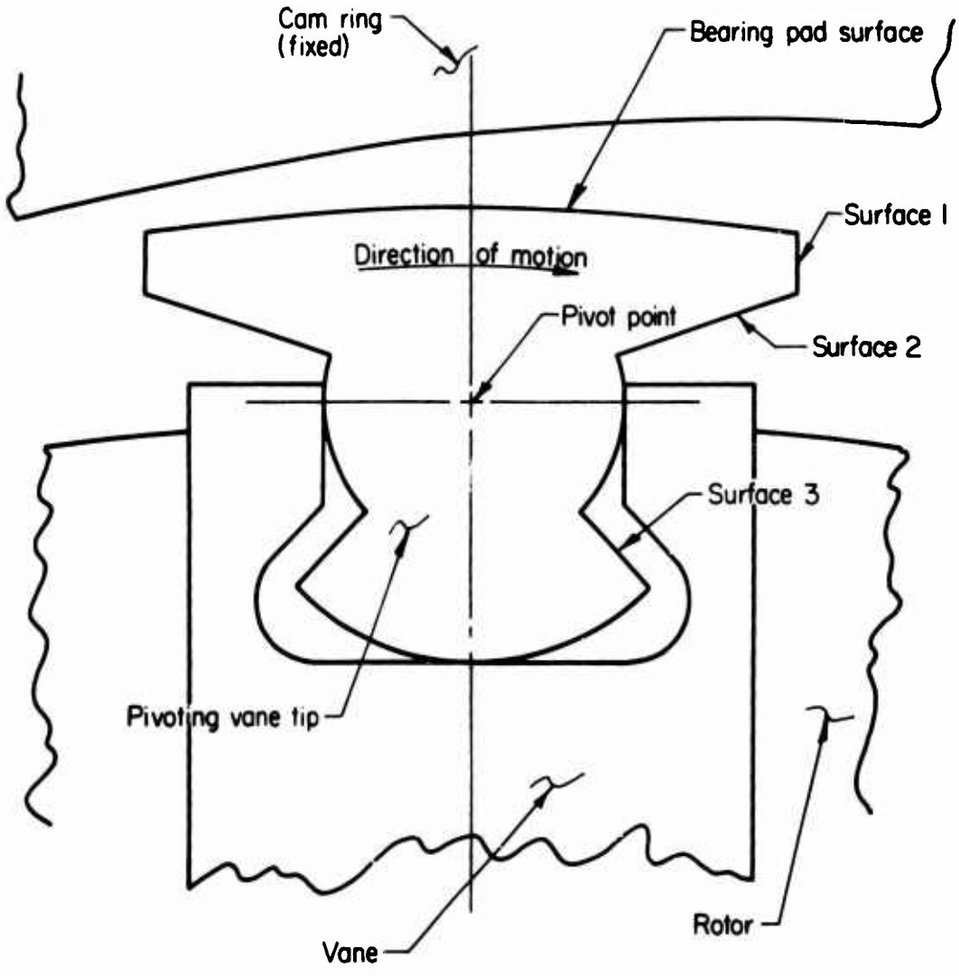

Figure 16. Generalized Pivoting Vane-Tip Configuration.

to 120 microinches on the critical sealing lap space at the light-off conditions. The increased bearing pad width would provide approximately 50 percent more load support and a 10-microinch increase in the theoretical minimum film thickness at 50,000 rpm with a vane stage differential pressure of 700 psi.

In addition to the operational improvements, this vane-tip design simplifies the fabrication of the vane. The extension of Surface 3 provides stops to encapsulate the tip in the vane. This insures that tip/vane separation does not occur during startup. The present vane socket technique used to insure encapsulation requires close tolerances not necessary with the new design. The vane slot for the tip can also be ground from the end, a much more simple task than producing the present round vane socket. The improved rotational stiffnes of the tip bearing also allows for a relaxation in the tip tolerances, for an exact control of the pressure balancing areas is not necessary to obtain proper stability.